HHS Public Access

Repeated Stress Induces a Pro-inflammatory State, Increases Amygdala Neuronal and Microglial Activation, and Causes Anxiety in Adult Male Rats

Soumyabrata Munshi[1,2], **Maxine K. Loh**[1,4], **Nicole Ferrara**[1,4], **M. Regina DeJoseph**[3,4], **Alexandra Ritger**[2,4], **Mallika Padival**[1,4], **Matthew J. Record**[1], **Janice H. Urban**[3,4], **J. Amiel Rosenkranz**[1,4,*]

[1]Department of Foundational Sciences and Humanities, Cellular and Molecular Pharmacology, Rosalind Franklin University of Medicine and Science, 3333 Green Bay Road, North Chicago, IL 60064, USA.

[2]Department of Foundational Sciences and Humanities, Neuroscience, Rosalind Franklin University of Medicine and Science, 3333 Green Bay Road, North Chicago, IL 60064, USA.

[3]Department of Foundational Sciences and Humanities, Physiology and Biophysics, Rosalind Franklin University of Medicine and Science, 3333 Green Bay Road, North Chicago, IL 60064, USA.

[4]Center for Neurobiology of Stress Resilience and Psychiatric Disorders, Rosalind Franklin University of Medicine and Science, 3333 Green Bay Road, North Chicago, IL 60064, USA.

Abstract

A link exists between immune function and psychiatric conditions, particularly depressive and anxiety disorders. Psychological stress is a powerful trigger for these disorders and stress influences immune state. However, the nature of peripheral immune changes after stress conflicts across studies, perhaps due to the focus on few measures of pro-inflammatory or anti-inflammatory processes. The basolateral amygdala (BLA) is critical for emotion, and plays an important role in the effects of stress on anxiety. As such, it may be a primary central nervous system (CNS) mediator for the effects of peripheral immune changes on anxiety after stress. Therefore, this study aimed to delineate the influence of stress on peripheral pro-inflammatory and anti-inflammatory aspects, BLA immune activation, and its impact on BLA neuron activity. To produce a more encompassing view of peripheral immune changes, this study used a less restrictive approach to categorize and group peripheral immune changes. We found that repeated social defeat stress in adult male Sprague-Dawley rats increased the frequencies of mature T-cells

[*]**Corresponding Author:** J. Amiel Rosenkranz, Ph.D., Center for Neurobiology of Stress Resilience and Psychiatric Disorders, Rosalind Franklin University of Medicine and Science, 3333 Green Bay Road, North Chicago, IL 60064, USA., Telephone: 847-578-8680; Fax: 847-578-3268, jeremy.rosenkranz@rosalindfranklin.edu.

positive for intracellular type 2-like cytokine and serum pro-inflammatory cytokines. Principal component analysis and hierarchical clustering was used to guide grouping of T-cells and cytokines, producing unique profiles. Stress shifted the balance towards a specific set that included mostly type 2-like T-cells and pro-inflammatory cytokines. Within the CNS component, repeated stress caused an increase of activated microglia in the BLA, increased anxiety-like behaviors across several assays, and increased BLA neuronal firing *in vivo* that was prevented by blockade of microglia activation. Because repeated stress can trigger anxiety states by actions in the BLA, and altered immune function can trigger anxiety, these results suggest that repeated stress may trigger anxiety-like behaviors by inducing a pro-inflammatory state in the periphery and the BLA. These results begin to uncover how stress may recruit the immune system to alter the function of brain regions critical to emotion.

Keywords

Basolateral amygdala; Behavior; Cytokines; *In vivo* electrophysiology; Microglia; Social defeat stress; T-cells

1. Introduction

Chronic psychological stress is one of the most common triggers of clinical depression, causing lasting anxiety, depressed mood and other symptoms (van Praag, 2005; Bartolomucci and Leopardi, 2009). These psychiatric symptoms and experience of stress are both associated with alterations of the immune system, suggesting that, in some cases, stress may trigger depression and anxiety via effects on the immune system. The immune system may exert this effect through white blood cells, particulalrly T-cell populations of lymphocytes and monocytes, as well as cytokines that mediate cell-to-cell communication (Dantzer, 2001; Anisman and Merali, 2002; Konsman et al., 2002; Kiecolt-Glaser et al., 2003; Wohleb and Delpech, 2017). Mature T-cells are characterized as either CD4+ helper (Th) or CD8+ cytotoxic (Tc) T-cells. T-cells are either pro-inflammatory (type 1) or anti-inflammatory (type 2) depending on the predominant types of cytokines secreted. T-helper (Th)-1 cells secrete mainly pro-inflammatory cytokines whereas the Th-2 cells mainly secrete anti-inflammatory cytokines (Mosman and Sad, 1996). Regulatory T-cells (Treg cells) are a specialized subset of CD4+ T-cells that suppress potentially deleterious effects of Th cells (Corthay, 2009). The relative balance of different types of T-cells greatly influence the inflammatory state.

There is strong evidence that stress can impact T-cell populations in humans, a major source of peripheral cytokines. Psychological stress in humans is associated with an increased accumulation of peripherally primed monocytes with higher potential for inflammatory signaling as evidenced by increased pro-inflammatory-related gene expression (Miller et al., 2008; Cole et al., 2011; Powell et al., 2013), with subsequent increase of cytokines (Kiecolt-Glaser et al., 2003; Hou et al., 2017), particularly those categorized as pro-inflammatory interleukins (IL), IL-6, IL-1β, and IL-10. Similarly, meta-analysis of patients with stress-related psychiatric disorders, such as depression or post-traumatic stress disorders, indicate a picture of increased pro-inflammatory cytokines (Tursich et al, 2014; Passos et al, 2015;

Breen et al, 2018; Renna et al, 2018). However, meta-analyses find variability in the effects of stress on T-cell populations, with some evidence pointing towards a reduction of Th-1 and Th-2 cells and other findings suggesting a shift from Th-1 to Th-2 cells (Segerstrom and Miller, 2004; Nakata, 2012). Furthermore, the effects of stress on peripheral cytokines does not follow a pattern that would be predicted for a simple general increase in Th1 or Th2 cell function (e.g. Maes et al., 1998; Kamezaki et al., 2012). Indeed, not all studies find increased type 1 pro-inflammatory profiles, some studies find a decrease, and others highlight the importance of changes in type 2 profiles (Nakano et al., 1998; Kaufman et al., 2007). While meta-analyses support an effect of stressors on several pro-inflammatory cytokines in healthy individuals (Segerstrom and Miller, 2004; Marsland et al, 2017), there is also strong evidence for increased anti-inflammatory cytokines (Marsland et al, 2017) or decreased pro-inflammatory cytokines (Eddy et al, 2016) in healthy individuals, and there is some heterogeneity in the exact pattern of changes across individual studies

One way to understand discrepencies across studies is recognition that a clear picture might not emerge upon examination of a single cytokine, or small group of cytokines. Instead, better insight might be gained by examining the balance between different groups of cytokines. However, even studies that assess a balance between pro- and anti-inflammatory cytokines, measured as the ratio between a chosen pro- and anti-inflammatory cytokine, have produced variable results (Hashizume et al, 2005; Rehm et al, 2013; Karlsson et al, 2017). The differences in these effects of stress on cytokine profiles could be due to differences in the populations studied, stressor examined, and measures used. This highlights the need for a comprehensive set of measures from the same stressor under the same conditions. Another likely factor is that the immune response includes a number of cytokines that interact dynamically. A broader understanding of the effects of stress may be achieved by examination of a wider number of cytokines and how they co-vary.

Substantially more is known about immune system states following stress in animal models. Chronic stress increases neutrophils and monocytes output in circulation (Powell et al., 2013; Heidt et al., 2014), consistent with greater capacity for inflammatory responses. While more studies have supported an increase of pro-inflammatory cytokines after acute or repeated stress, similar to studies in humans, animal models show a variable shift from type 1 and type 2 cytokine profiles after stress, with findings of increased Th1 cytokines or reduced Th2 cytokines (Bartolomucci et al, 2001; Chida et al, 2005; Savignac et al, 2011; Azzinnari et al., 2014; Stewart et al, 2015) or even decreased Th1 or increased Th2 cytokines (Mormède et al, 2002; Hou et al., 2013; Ahmad et al., 2015; Hu et al., 2016) perhaps depending partly upon which of the diversity of stressors were used (Deak et al., 2003; Deak et al., 2005; Bowers et al., 2008; Hueston et al., 2011; Shaashua et al., 2012; Budiu et al., 2017), or on which cytokines are measured. Therefore, it is important to examine a range of both pro-inflammatory and anti-inflammatory cytokines, along with T-cell populations to fully understand the effects of a specific stressor on the peripheral immune system, and to understand how a balance between cytokines might shift. However, the categorization of cytokines into pro-inflammatory or anti-inflammatory is somewhat artificial, with now established evidence for overlap in the inflammatory effects of type 1 and type 2 cytokines. Therefore, even if using classical pro-inflammatory and anti-inflammatory cytokines as a starting point for analysis, an unbiased characterization of the

balance between different cytokine groups is important to test. This is expected to produce a more accurate reflection of the effect of stress on the peripheral immune environment, and may spark exploration of new avenues to interfere with the harmful effects of stress. Thus, one goal of this study is to use a rodent model to test if repeated stress causes an imbalance of the peripheral inflammatory state using an approach that does not focus on any single cytokine, or any pre-determined group of cytokines, but instead determines how the balance between groups of covarying cytokines changes.

While many immune changes might be initiated in the periphery, immune changes in the central nervous system (CNS) likely produce some of the behavioral outcomes caused by stress (Wohleb et al., 2013; McKim et al., 2018; Wohleb et al., 2018). Microglia are the resident immune cells of the CNS (del Rio-Hortega, 1932; Ginhoux et al., 2010; Ginhoux et al., 2013) with density ranging from 5% to 12% of the total number of cells in different brain regions (Lawson et al., 1990). Acute and chronic stress produce microglia activation in the prefrontal cortex, amygdala, and the hippocampus (Sugama et al., 2009; Tynan et al., 2010; Wohleb et al., 2012), which can contribute to the development of anxiety and depressive behavior after chronic stress (Wohleb et al., 2013; McKim et al, 2018; Wohleb et al., 2013). The basolateral amygdala (BLA) is a primary region involved in stress-induced anxiety. Chronic stress strongly increases BLA neuron activity and impacts morphology (Vyas et al, 2002; Rosenkranz et al., 2010; Zhang and Rosenkranz, 2012). The BLA may be impacted by the effects of stress on immune function, and activation of BLA microglial cells would be a fairly direct route. Indeed, chronic social defeat stress in mice altered immune signaling genes in the amygdala (Azzinnari et al., 2014). However, the effects of chronic stress on BLA microglia are not clear, with evidence that repeated restraint stress in male rats reduces the proportion of primed to surveillant microglia (Bollinger et al., 2017) or has no effect on microglia number and morphology (Tynan et al, 2010), with differences perhaps related to duration of the stress exposure and related habituation to the repeated stress. Social stressors exert a powerful, lasting impact on immune function in humans (Shimamiya et al., 1985; Gerritsen et al., 1996; Caserta et al., 2008; Miller et al., 2009; Slopen et al., 2015) and rodents (Stefanski and Engler, 1998; Stefanski et al., 2001; Dunphy-Doherty et al., 2018). One way to model this in rats is with repeated social defeat stress (RSDS). RSDS causes alterations that parallel psychiatric symptoms after stress, characterized by increased anxiety, social-avoidance, and anhedonia (Rygula et al., 2005; Berton et al., 2006; Rygula et al., 2006). Additionally, RSDS is known to have a robust effect on immune parameters in rodents (Wohleb et al., 2013), and these immune changes are required to produce RSDS effects on anxiety (Wohleb et al., 2011; Wohleb et al., 2013). Despite robust effects of social stress on immune function, it remains untested if social stress impacts BLA microglia activation. Thus, one goal of this study is to test the effect of repeated stress on microglia and neuronal activity in the BLA, and whether disruption of microglia activation can prevent the effects of stress on BLA neuronal activity. The BLA is comprised of multiple nuclei that have distinct roles in behavior, most notably the lateral (LAT) and basal (BA) nuclei, and it is important to consider both nuclei of the BLA.

In this study we used RSDS to explore how repeated social stress impacts the peripheral immune balance by measuring how peripheral immune precursor and mature T-cells and serum cytokines co-vary. To achieve this, we used an unbiased approach to group T-cell

profiles and cytokines, and measured the effects of stress on the balance between these groups. We also examined parallel effects of repeated social stress on a CNS site important in anxiety, by measuring BLA-sensitive anxiety behaviors, BLA microglia number and activation, BLA neuronal activity , and whether blockade of microglia activation alters the effects of stress on BLA neuron activity.

2. Materials and Methods

2.1. Ethical approval and animal subjects

All experiments were performed in compliance with the Guide for the Care and Use of Laboratory Animals (National Research Council, 2011) and were approved by the Institutional Animal Care and Use Committee (IACUC) of Rosalind Franklin University of Medicine and Science. Care was taken to reduce the total number of animals used for the study. Adult male Sprague-Dawley rats (Envigo, Indianapolis, IN) were obtained at post-natal day 59–63 and were housed 2–3 per cage in the climate-controlled Biological Resource Facility at Rosalind Franklin University of Medicine and Science with *ad libitum* access to food and water. After habituating in the animal facility for at least 4 days, rats were subjected to stress or control handling. Lights in the housing room were on a reversed 12h light / dark schedule (light off: 07:00–19:00). Only male rats were used in the study because the social defeat stress model using aggressive male rats is not compatible with female rats. A version of social aggressive stress can be imposed on female rats using aggressive lactating female rats (Ver Hoeve et al, 2013), but most of the female intruder rats received a scratch or bite wound during exposure to the aggressive female in preliminary studies. This wound, even though small, could introduce a significant confound that impacts immune measures. A total of 149 rats were used in the study (43 for behavior, 24 for FACS, 28 for ELISA, 12 for immunohistochemistry and 42 for electrophysiology experiments). Adult male retired breeder Long-Evans rats were used to induce social defeat stress to the Sprague-Dawley rats. Rats were randomly assigned to groups, experiments were performed in multiple cohorts, and experimenters were blinded to treatment groups whenever possible.

2.2. Induction of repeated social defeat stress

Repeated social defeat stress (RSDS) by resident-intruder sessions is a robust model of chronic psychological stress in rodents (Rygula et al., 2005; Berton et al., 2006; Liu et al., 2017). Cages of rats were randomly assigned to the stressed and control groups. The experimental intruder was weighed before being introduced into the home cage of an unfamiliar "resident" (aggressive adult male retired breeder Long-Evans rat) daily for five consecutive days, in a dimly lit behavioral room free from noise within the animal facility. The rats were allowed to stay in direct physical contact with each other in the resident cage for a maximum of 15 min each session, after which the intruder was separated within the resident's cage using a wire mesh box for an additional 15 min. During the period of direct physical contact, every attack made by the aggressor rat on the intruder was scored manually by a trained observer, including noting the time of first attack and the time of physical separation. A defeat happened when the intruder rat submitted to the attack of the aggressor by lying down and exposing the ventral surface (abdomen). The wire mesh box used for physical separation was spacious enough not to cause any form of physical restraint to the

movements of the rat inside. The experimental rat was separated with the mesh box prior to 15 min if any of the following criteria was met: (i) submission of the intruder; (ii) 10 attacks with no submission; (iii) 5 min with no attack; or (iv) any attack that severely wounded the experimental rat. Thus, not every rat was socially defeated every day, however, each rat demonstrated submission over the course of the 5 days. In the control group, rats were weighed daily in the morning for five consecutive days and were placed in transport cages for 30 min before they were returned to their home cage. The primary focus of this study was the persistent effects of repeated stress. Therefore, experiments and blood collections were done 48 hours after the last stress/handling session to avoid acute short-lived effects of social defeat.

2.3. Behavioral experiments

Behavioral experiments were performed to measure the anxiety-like state induced by the RSDS. The order of behavioral tests was (1) open field test, (2) social interaction test, (3) elevated plus maze test, when applicable.

2.3.1. Open field test—The open field (black opaque, 24 in. × 35 in.) test was performed in a dimly lit room (20–25 lx) with computer-generated white noise (65–70 dB) for 5 min. Behavioral recordings were obtained using IR-sensitive cameras (Fire-i, Unibrain, San Ramon, CA) connected to a computer (Dell E6500, Round Rock, TX) and were saved for off-line analysis using ANY-Maze version 4.99 z (Stoelting, Wood Dale, IL). The field was thoroughly cleaned with 70% ethanol between rats. The total distance traveled and central area exploration in the field was quantified and compared.

2.3.2. Social interaction test—A novel adult male Sprague-Dawley rat, weighing within 50 g of the test rat, was introduced in the field and rats were allowed to interact with each other for 5 min. The novel rat had previously been introduced in this open field for at least 10 min. The trunk of the test rat was marked with black ink for identification during the test. Socially interactive behaviors were defined by sniffing (body and anogenital), close following, pushing the head or snout under the novel rat's body, crawling over (or under), or boxing (or wrestling), as described previously (File and Hyde, 1978; Vanderschuren et al., 1997; Varlinskaya and Spear, 2008; Boschen et al., 2014). The number of times the test rat approached and interacted with the novel rat was quantified from the recorded video by a trained rater. The rater showed a consistent > 90% similarity in tabulations before all final data were collected. The total time of interaction was also quantified during a separate video replay using a digital stop-watch.

2.3.3. Elevated plus maze test—The elevated plus maze (EPM; Scientific Designs, Pittsburgh, PA) consisted of four arms: two open arms (width × length: 5 in. × 20 in.) and two closed arms (width × length × wall height: 5 in. × 20 in. × 18 in.). Each arm was attached to a leg stand, elevated 32 in. from the ground. The rats were individually placed at the junction of the four arms, facing the open arm opposite the experimenter. Rat behavior was recorded for 5 min with video-tracking software (ANY-Maze, Stoelting, Wood Dale, IL) and was saved for future analysis on a computer (Dell E6500). The time spent on open arms was measured and used as an index of anxiety-like behavior. Additionally, the number of

total arm entries and total distance traveled in EPM were measured to use as an indicator of locomotor activity.

2.4. Fluorescence-activated cell sorting (FACS) / flow cytometry

To avoid potential effects of wounds on measures of peripheral inflammation, any rat that was wounded during social stress was excluded from peripheral measures of T-cells or cytokines. Rats were anesthetized with urethane (1.5 g / kg dissolved in 0.9% saline, i.p.; Sigma-Aldrich, St. Louis, MO) and peripheral blood was collected (decapitation within 15 – 30 mins of injection of anesthesia) in sterile heparinized tubes. Urethane was used to anesthetize rats for all measures that can change rapidly, such as cytokines and T-cells, to match electrophysiology experiments that use urethane to provide long-term stable recordings. FACS was done following previously published methods (Berner et al., 2000; Lutgendorf et al., 2008; Ahmad et al., 2015). All reagents and antibodies were obtained from BD Biosciences (San Jose, CA) unless mentioned otherwise. Gating was done for each antibody based on the non-specific binding of the appropriate negative isotype stained controls (Wohleb et al., 2012).

2.4.1. Determination of T-cell count frequencies—Briefly, 2.5 μL each of BV421 mouse anti-rat CD3 (Catalog No. 563948), PE-Cy7 mouse anti-rat CD4 (Catalog No. 561578) and FITC mouse anti-rat CD8a (Catalog No. 561965) antibodies were added to 100 μL of the heparinized blood and incubated at room temperature for 15 min. Respective isotype antibodies (IgG1, IgG2 and IgMκ) were added to another 100 μL of the corresponding heparinized blood and incubated similarly; these were used as the respective isotype controls. Red blood cell lysing buffer (2 mL, containing ammonium chloride, potassium bicarbonate and EDTA; all from Sigma-Aldrich; pH 7.65) was added to each tube, and they were incubated for 15 min at room temperature in the dark. The mixture was then centrifuged at $200 \times g$ for 5 min at 4°C (IEC Centra – 7R Refrigerated Centrifuge, Rochester, NY) and the supernatant was discarded. FACS staining buffer (1 mL) was then added, the mixture was again centrifuged at $200 \times g$ for 5 min at 4°C and the supernatant was discarded. The final pellet was suspended gently and uniformly in 500 μL FACS staining buffer and analyzed immediately by flow cytometer (LSR II, BD Biosciences). Multicolor flow cytometric analysis of T-cell surface markers and intracellular IFN-γ or IL-4 expression was performed. Single cell suspensions were gated for CD3+ which marked the T-cell population. That was further gated for CD4+ and CD8+ labels. Samples were then analyzed for percentages of dual negative (DN, CD4−CD8−), dual positive (DP, CD4+CD8+), CD4+ and CD8+ T-cells by flow cytometer (LSR II, BD Biosciences). 10,000 events were captured during acquisition per treatment condition and data was stored. Analyses were done using FlowJo FACS software. T-cells were defined as CD3+ cells (Lutgendorf et al., 2008), and were further divided into CD3+CD4+ (helper T-cells or Th-cells) and CD3+CD8+ (cytotoxic T-cells or Tc-cells).

2.4.2. Intracellular cytokine staining (ICS)—For ICS study, blood was similarly processed as described above with slight modifications as follows: After the first centrifugation at $200 \times g$ for 15 min at 4°C, the supernatant was discarded and 500 μL of fixation/permeabilization buffer was added and incubated for 10 min at room temperature in

the dark. This was followed by addition of 4 mL of wash buffer (containing 10 μL of Fc blocking solution and 40 μL GolgiPlug protein transport inhibitor with brefeldin A). This was let to stand for 10 min followed by centrifugation (200 × g for 5 min at 4°C). After the final suspension of the pellet in 500 μL FACS staining buffer, the cytokine-specific Alexa Fluor 647 mouse anti-rat IFN-γ (Catalog No. 562213) and PE mouse anti-rat IL-4 (Catalog No. 555082) antibodies were added and incubated for 30 min before analysis by FACS (LSR II, BD Biosciences). The corresponding isotype controls were used simultaneously. A minimum of 5,000 events were captured during acquisition per treatment condition. Analyses were done later using FlowJo FACS software when the percentages of intracellular Th1 (or Tc1)- and Th2 (or Tc2)-like cytokine-positive DN, DP, CD4+ and CD8+ T-cells were calculated. Type-1 and Type-2 responses were defined by expression of IFN-γ and IL-4 by the cells, respectively.

2.4.3.   Determination of Treg-cell count frequencies—Treg cell staining was done using the rat regulatory T-cell multi-color flow cytometry kit (R&D Systems, Minneapolis, MN; Catalog No. FMC015) Briefly, 2.5 μL of BV421 mouse anti-rat CD3 (BD Biosciences; Catalog No. 563948), 10 μL of CD4-FITC, 10 μL of CD25-PE and 10 μL of FoxP3-APC antibodies or isotype controls were added to 100 μL of the heparinized blood and incubated at room temperature for 15 min before analysis by FACS (LSR II, BD Biosciences). Treg cells were defined as CD4+CD25+FoxP3+ T-cells.

2.5.   Quantification of serum cytokines with ELISA after RSDS

Similar to blood collection for FACS experiments, rats were anesthetized with urethane (1.5 g / kg dissolved in 0.9% saline, i.p.) and peripheral blood was collected in sterile tubes by decapitation within 15 – 30 mins of injection of anesthesia. Blood remained at room temperature for 30 min and was then centrifuged at 1000 × g for 15 min at 20°C. Sera samples were stored at −80°C until ELISA was performed following kit literature (MER-004A, Qiagen, Germantown, Maryland, USA). Briefly, experimental controls and diluted serum samples were added to appropriate wells of the ELISArray plate pre-coated with capture antibodies and incubated for 2 h. This was followed by washing away the unbound proteins and adding biotinylated detection antibody and incubating for 1 h. After washing the unbound materials again, avidin-horseradish peroxidase conjugate was added. This was incubated for 30 min followed by washing and incubation in development solution for 15 min in the dark. The color development reaction was stopped by addition of stop solution and absorbance was read at 450 nm with wavelength correction set at 570 nm. After adjusting for the dilution factor of the samples used, group difference in the ratio of absorbance was calculated as the fold increase ($[samples]_{RSDS}$ / $[average]_{CONTROL}$).

2.6.   Immunohistochemistry for detection of microglia in BLA after RSDS

Tissue processing and immunohistochemistry were performed following earlier published methods (Urban et al., 2006; Leitermann et al., 2016; Woitowich et al., 2016). Briefly, rats were anesthetized with pentobarbital (100 mg/kg, i.p., Sigma-Aldrich) and were perfused transcardially with phosphate-buffered saline (PBS; 37°C) containing 0.1% procaine and heparin, and immediately followed by ice-cold 4% paraformaldehyde in PBS (pH 7.5). Urethane was not necessary to use in this instance because the number of microglial cells in

the brain is not expected to change on a rapid time scale and therefore less likely to be sensitive to anesthesia type in the short time between induction and euthanization. At the end of perfusion, the brains were gently removed and stored in fixative at 4°C overnight. The brains were transferred to PBS and stored at 4°C until sectioning with a vibratome (40 μm; Ted Pella, Inc., Redding, CA).

Immunohistochemsitry for Iba-1—On the day of immunohistochemistry, sections were rinsed in PBS (pH 7.4), treated with 1% hydrogen peroxide (H_2O_2) for 15 min, and further rinsed in 3×5 min PBS washes. The sections were blocked for 3 h in 10% normal donkey serum (NDS) in PBS-gelatin and then incubated for 72 h in primary ionized calcium binding adaptor protein - 1 (Iba-1) antibody (1:2,000; Wako Chemicals, Richmond, Virginia) in buffer containing 5% NDS and 0.2% Triton X-100 (Catalog No.: 807426, MP Biomedicals, Santa Ana, CA). After incubation, the sections were rinsed in PBS-gelatin and incubated in biotinylated donkey anti-rabbit antibody (1:750) for 1 h. After washes in PBS, the tissues were incubated in avidin-biotin complex (2 μL / mL; ABC reagent; Vector Laboratories, Burlingame, CA) for 30 min and rinsed in PBS-gelatin. Sections were mounted on gelatin-subbed slides and air dried. Coverslips were applied using mounting medium.

Double label immunohistochemistry for Iba-1 and CD68—To determine the expression of CD68 immunoreactivity within Iba-1-immunopositive microglia, double label immunohistochemistry was used as described previously (Rostkowski et al., 2009). CD68 immunoreactivity within sections of the BLA were visualized using biotinylated tyramide amplification immunofluorescence. Briefly, free-floating sections were rinsed through 3 changes of PBS over 10 minutes, followed by a 15 min wash in 1% H_2O_2 in PBS to diminish endogenous peroxidase activity. Next, tissues were blocked for 3 hours in immunocytochemistry (ICC) buffer (0.1 M PBS containing 0.2% gelatin, 0.01% thimerosal and 0.002% neomycin, pH 7.5) containing 0.01% TritonX-100 and 5% normal donkey serum (NDS; Equitech-Bio, Kerrville, TX) to block non-specific binding. Sections were then incubated at +4°C for 72 hours with anti-CD68 antibody (1:1000; Bio-Rad Laboratories, Mouse) in ICC with 2% NDS and 0.01% TritonX-100. Following incubation with primary antibody, sections were washed through 5 changes of ICC buffer over 50 minutes and then incubated with biotinylated, affinity purified donkey anti-rabbit IgG (Jackson ImmunoResearch Laboratories, Inc., West Grove, PA; 1:2,000) for 1hr at room temperature. After ICC buffer rinses, sections were incubated in Vectastain Elite ABC (Vector Laboratories, Burlingame, CA; 2 μL/mL) for 30 minutes. Next, sections were rinsed with PBS and incubated in biotinylated tyramide solution (3 μg/mL biotinylated tyramide and 0.01% H_2O_2 in PBS) for 10 minutes. Tissues were then rinsed in ICC buffer and immersed in ICC buffer containing fluorescein isothiocyanate conjugated streptavidin (FITC-SA; Jackson ImmunoResearch Laboratories, Inc., West Grove, PA; 1:250) for 3 hours. Following washes in 4 changes of tris-buffered saline (TBS: 100 mM Tris base, 150 mM NaCl, pH 7.5) over 20 minutes, sections were incubated with anti-Iba-1 (1:1000; 48 hrs). Sections were subsequently washed through 5 changes of ICC buffer over 50 minutes followed by a 3 hour incubation in ICC buffer containing Cy3 donkey anti-mouse secondary antibody (Jackson ImmunoResearch Laboratories, Inc., West Grove, PA; 1:250). Following 2 rinses in TBS, sections were mounted onto Superfrost+ slides and coverslips were applied with 2.5%

polyvinyl alcohol-1,4-diazabicyclo[2.2.2]octane (PVA-DABCO) anti-fade mounting medium.

2.7. Counting of microglia in the BLA

The number of microglia in BLA sections were counted as Iba-1-positive cells using a comparable number of sections from rats across groups (Control: total 33 sections / 6 rats from −2.16 mm to −3.36 mm from bregma; RSDS: total 36 sections / 6 rats from −2.28 mm to −3.36 mm from bregma) following earlier published methods (Yin et al., 2010; Morrison et al., 2017). Images were acquired at 20X objective lens magnification and were later opened with ImageJ software where the border of the BLA was delineated. The microglia numbers within the confines of the BLA were then counted manually by an observer blind to treatment history of individual sections. This gave the number of microglia/section. These were averaged per section and compared between groups. The borders of the LAT and BA nuclei within the BLA were also delineated. The data were subdivided into those within the BA and the LAT nuclei of the BLA. The morphology of the microglia was also closely examined at 20X, 40X and 100X objective lens magnification, and the number of cells were calculated (expressed in percentage of total number of microglia) in the following three groups: (a) Group I (ramified) microglia which had long processes but small cell body size, (b) Group II (intermediate) microglia which had smaller processes but comparatively larger cell body size, and (c) Group III (ameboid) microglia which were ameboid in shape with no processes. During activation, the morphology of the microglia changes from resting ramified to the ameboid forms along with increased expression of Iba-1 (Stence et al., 2001; Beynon and Walker, 2012).

Quantification of immunostained cells in tissues that were labeled with multiple fluorescent markers (Iba-1 and CD68) was performed for BA and LAT nuclei. Sections were analyzed using scanning laser confocal stereology. Images of the BLA were captured at 10x magnification and the borders of the nucleus were manually outlined for each section using Olympus Fluoview 300 microscope (Olympus, Melville, NY) equipped with a motorized x-y-z stage control. Reprsentatitve atlas-matched sections were taken for analysis for a total of 4 sections throughout the rostral-caudal extent of the nucleus (from bregma −1.8 mm to bregma −3.30 mm) according to Paxinos and Watson (1998). Two (LAT) or three (BA) counting frames (200 μm × 200 μm) were generated per brain region. At each systematic randomly selected site, a serial confocal stack of each fluorophore was individually captured on the appropriate emission channel using a 60x oil immersion objective (1.4 numerical aperture). The following excitation wavelengths were used: 488 nm for the secondary fluorophore FITC, 568 nm for Cy3. Stacks were then merged and saved for counting offline. Colocalization was determined by observing overlapping signals at several focal planes though each cell by experimenters blinded to the treatment groups. Only cells whose complete cell body was within the inclusion limits of the counting frames were counted. Total cell number of single Iba-1 and double labeled cells was counted and reported as percent co-expression per total Iba-1 cells counted.

2.8. *In vivo* extracellular single-unit electrophysiology

In order to examine the effect of the repeated stress on the spontaneous firing of the BLA neurons, *in vivo* extracellular, single-unit, spontaneous neuronal firing was recorded following earlier published methods (Zhang and Rosenkranz, 2012) from a separate cohort of rats that underwent the RSDS or control handling. Briefly, the rats were anesthetized with urethane (1.5 mg/kg, i.p.) and placed in stereotaxic apparatus (David Kopf Instruments, Tujunga, CA). Rats were maintained at approximately 37°C (TC-1000 Temperature Controller, CWE Inc, Ardmore, PA) and burr holes were drilled in the skull overlying the BLA. Anesthesia depth was confirmed by lack of response to foot pinch and by primary rhythmicity of local field potentials between 0.51.5 Hz. Glass pipettes (borosilicate 2.0 mm o.d., World Precision Instruments Inc, Sarasota, FL) were heat-pulled (PE-2 puller, Narishige, Tokyo, Japan), tips broken back to approximately 1 μm, and filled with 2% Pontamine Sky Blue in 2 M NaCl. Recording electrodes were lowered slowly into the BLA (−2.5 to −3.6 mm caudal and −4.4 to −5.1 mm lateral from bregma) and signals were amplified and filtered (1.0 Hz – 5 kHz, Model 1800 Microelectrode Amplifier, A-M Systems, Sequim, WA), monitored visually (2120 oscilloscope, B and K Precision, Yorba Linda, CA) and audially (AM10 Audio Monitor, Grass Instruments, Warwick, RI). Signals were digitized (HEKA ITC-18, Holliston, MA) and saved for analysis (AxoGraph × version 1.6.4, Sydney, Australia) on a Mac Pro computer (Apple Inc, Cupertino, CA). At the conclusion of recordings, Pontamine dye was ejected from the recording electrode by constant current (−30 μA, Constant Current Source, Finntronics, Orange, CT) for at least 30 minutes. Rats were decapitated, brains were removed and placed in 4% paraformaldehyde with 0.05% potassium ferrocyanide in 0.1M phosphate buffer for greater than 12 hours and then transferred to 25% sucrose in 0.1M phosphate buffer until sectioning. Brains were sliced into 60 μm sections with a freezing microtome (Leica Microsystems Inc., Wetzlar, Germany) and then Nissl stained. Recording sites were verified by light microscopy and reconstructed using a rat brain atlas (Paxinos and Watson, 2007). To meet inclusion criteria for analysis, neurons were verified to lie within the LAT or BA, there was a clear signal : noise (> 3 : 1), and a continuous 4 min stable recording (with consistent action potential amplitude) was obtained.

In a separate set of experiments, the role of microglia in establishment of the effects of stress on BLA neuron firing was measured using the social defeat design, as described above. In addition, rats were treated with a blocker of microglia activation, minocycline (Hello Bio, Bristol, UK; 40 mg/kg i.p. in saline, 2 mL/kg body weight) or saline control, 60 min prior to each social defeat stress. This dose of minocycline was chosen based on previously established effects on microglia activation (Blandino et al, 2006). Rats were prepared for electrophysiology after 48 hours (range 48 – 96 hrs). All rats with recordings of BLA neurons that met inclusion criteria (mentioned above) were included for analysis.

2.9. Data analysis

Statistical analysis was performed using Microsoft Excel (Redmond, WA) and GraphPad Prism version 6.0h or 8.0.2 (La Jolla, CA). Data distribution was tested using the D'Agostino and Pearson omnibus normality test ($\alpha = 0.05$). For comparison between two groups, unpaired *t*-test or Mann-Whitney *U* test was performed as appropriate. For

determining significant main effects and interactions between main factors (treatment × morphology) on microglia, analysis of variance (ANOVA) was performed. When appropriate, Bonferroni's multiple comparisons test was performed after ANOVA. Statistical significance was set at $p < 0.05$. When noted, effects with $p = 0.050 – 0.071$ were identified as possible effect trends.

One goal of the study was to understand the balance between different types of immune responses, and the impact of stress on these measures. However, there are multiple functional ways to group T-cells and cytokines. To eliminate bias, we adopted a hypothesis-free exploratory data processing flow. Raw values were subjected to principal component analysis (PCA; BioVinci, BioTuring Inc) to determine whether groups of cytokines or T-cells tended to change together. This grouping was then confirmed with hierarchical clustering analysis (BioVinci, BioTuring Inc) using Ward's MISSQ method, chosen because of the non-binary and non-arbitrary data values. When appropriate, Pearson correlation matrices were constructed to further establish if these cytokines or T-cells tended to vary together. When these two approaches confirmed the grouping observed in PCA, groups were established of cytokine or T-cells. The values for each type of cytokine or T-cell in a group were normalized on a 0–1 value scale, and then summated for each individual sample to produce aggregate group measures. This step was necessary so that each cytokine or T-cell type can contribute equally to the aggregate group measure, and the data would not be skewed by T-cell to cytokines types that were in higher quantities. The ratio of each group was quantified for individual samples, and the correlation of each group and these ratios were tested for association with stress, quantified here as the number of attacks experienced. As above, multiple comparisons were adjusted using Bonferroni corrections.

3. Results

RSDS measures were obtained on each day of the stress exposure. Overall, rats were consistently attacked and submissions were displayed. The mean ± SEM of the number of attacks encountered by the defeated rats and the latency to submission are shown in Figure 1.

3.1. RSDS causes anxiety-like behavior

To verify the effectiveness of RSDS, anxiety-related behaviors were measured across several assays. Measures of locomotion were also obtained to allow appropriate interpretation of results.

3.1.1. Open-field test—RSDS caused a significant reduction in the central area distance traveled in the open field and time spent in the central area, compared to control (Figure 2A). There was no significant effects of RSDS on the total distance traveled (Figure 2A) in the open-field test. This is consistent with increased anxiety behavior without any locomotion disruption or injury that might interfere with interpretation.

3.1.2. Social interaction test—RSDS caused a significant reduction in the number of social interactions (Figure 2B) as well as the total time of social interactions (Figure 2B).

The duration of social interaction events was not affected by RSDS (Figure 2B). This is consistent with increased social anxiety behavior.

3.1.3. Elevated plus maze test—RSDS caused a significant reduction in the time spent in open-arms of the EPM, compared to the control (Figure 2C). Neither the total distance traveled (Figure 2C) nor the number of arm entries (Figure 2C) was different between RSDS and control groups. This is consistent with increased anxiety behavior in the EPM without any locomotor disruption. Overall, these behavioral results indicate that RSDS was an effective stressor in producing anxiety-like behavior without impacting locomotion. In addition, these measures of anxiety have been demonstrated to be sensitive to BLA changes. Therefore, this increase in anxiety may point to an impact on the amygdala.

3.2. RSDS differentially affects peripheral circulatory precursor and mature T-cells

Previous studies indicate that stress can impact several immune parameters. Changes in the peripheral immune system are often first observed in T-cells Therefore, we next examined the effect of RSDS on peripheral T-cell profiles.

3.2.1. T-cell frequency—RSDS caused an increase in the frequency of dual negative T-cells (Figure 3A upper left panel) and a decrease in dual positive T-cells (Figure 3A upper right panel). The frequency of mature CD4+ T-cells was significantly lower after RSDS compared to control (Figure 3A lower left panel) while mature CD8+ T-cells was similar (Figure 3A lower right panel). RSDS also decreased the frequency of Treg cells (Figure 3B). The decrease in dual positive T-cells could indicate decreased passage from dual negative to dual positive T-cells, or increased differentiation to CD4+ or CD8+ T-cells. We found that RSDS increased dual negative T-cells, suggesting the former, and decreased passage is leading to accumulation of dual negative T-cells.

Analysis of cell counts within the gates revealed that similar numbers of cells were counted between control and RSDS groups (CD3+ cells: Control 3896 ± 550.5, RSDS 3396 ± 673.4, $p = 0.29$; CD4+ T-cells: Control 2688 ± 361.4, RSDS 2164 ± 398.9, $p = 0.27$; Dual positive T-cells: Control 463.0 ± 121.9, RSDS 169.3 ± 73.84, $p = 0.53$; CD8+ T-cells: Control 644.8 ± 111.7, RSDS 652.1 ± 121.6, $p = 0.98$; Dual negative T-cells: Control 176.5 ± 75.71, RSDS 410.9 ± 130.7, $p = 0.62$). The values reflect the number of cells (Mean $\pm$ SEM) gated, not necessarily indicative of absolute or relative number of cells in treatment groups. The gating strategy is shown in Figure 3C. There was no significant correlation between the number of attacks to the defeated rats and the frequencies of the T-cells ($p > 0.05$ for all correlations; data not shown).

PCA analysis was performed on these cell populations. Based on PCA analysis, and confirmed with hierarchical clustering and correlation matrix (Figure 3D(i)), dual positive (DP) and Treg cells clustered together, while CD8+, CD4+, and dual negative (DN) cells were independent (Figure 3D(i) upper panel). DP and Treg cells were grouped together, forming a new aggregate group (Group 4), while the other cell populations remained separate (Groups 1–3). Repeated stress decreased Group 4 (Figure 3D(ii) upper left panel; $p = 0.0196$, t = 2.517, df = 22, two-tailed unpaired t-test). The relative balance between all groups (Group 4 (DP and Treg); Group 2 (CD8+); Group 1 (CD4+); Group 3 (DN)) was

quantified as the ratios between individual groups and compared between control and stress groups (Figure 3D(ii) upper right panel; stress × ratio interaction, $p = 0.0234$, $F(5,110) = 2.721$, two-way RM-ANOVA). The balance between DN cells:CD4+ cells and DN cells:Group 4 cells were shifted by repeated stress ($p < 0.05$, post hoc Bonferroni). Groups and ratios between groups were assessed for correlation with the number of attacks (Figure 3D(ii) lower panel). Neither the individual groups, nor the ratios between individual groups, significantly correlated with the number of attacks ($p > 0.05$ for all correlations between T-cell group and attacks, and between T-cell group ratios and attacks). These data suggest that the balance between DN cells relative to CD4+ cells and relative to Treg / DP cells is highly sensitive to stress. CD4+ T-cells coordinate the adaptive immune response by influencing the activity of other immune cells (Zhu et al., 2010; Tubo and Jenkins, 2014); thus their reduction suggests their possible involvement in the changes of cytokines and other immune dysregulation in our present study.

3.2.2. T-cell functional profiles—T-cells can be functionally characterized partly by their intracellular profile, as either Th1 or Th2, based on expression of either IFN-γ or IL-4. T-cells with these profiles were measured and the effects of stress were evaluated in Th1 and Th2 T-cells. Cells were then clustered and the balance between clustered groups were examined.

3.2.2.1.   Intracellular Th1 (or Tc1)-cytokine profile of T-cells: RSDS did not significantly impact frequency of any Th1 profile T-cells compared to control. This includes the frequency of dual negative T-cells positive for Th1 (IFN-γ) ICS (Figure 4A(i) left panel), frequency of dual positive T-cells positive for Th1 (IFN-γ) ICS (Figure 4A(ii) left panel), frequency of mature CD4+ T-cells positive for Th1 (IFN-γ) ICS (Figure 4(iii) left panel), and frequency of mature CD8+ T-cells positive for Tc1 (IFN-γ) ICS (Figure 4A(iv) left panel). The representative FACS images are shown in Figure 4B.

3.2.2.2.   Intracellular Th2 (or Tc2)-cytokine profile of T-cells: RSDS did not significantly impact the frequency of dual negative T-cells positive for Th2 (IL-4) ICS (Figure 4A(i) right panel) and frequency of dual positive T-cells positive for Th2 (IL-4) ICS (Figure 4A(ii) right panel) compared to control. However, RSDS increased the frequency of mature CD4+ T-cells positive for Th2 (IL-4) ICS (Figure 4(iii) right panel), and frequency of mature CD8+ T-cells positive for Tc2 (IL-4) ICS (Figure 4(iv) right panel) compared to controls. These changes are consistent with a type 2-like polarization of the mature (CD4+ and CD8+), but not the immature (dual negative and dual positive), T-cells after RSDS. The representative FACS images are shown in Figure 4B.

There were no significant correlations between any of the Th1 cell types and attacks, nor Th2 cell types and attacks ($p > 0.05$ for all correlations, data not shown). PCA and hierarchical clustering was performed to discover whether any groups clustered (Figure 4C(i)). Three clusters emerged: Group 1 [CD8+ IL-4, CD4+ IL-4, DN IL-4, DP IFN-γ], Group 3 [CD8+ IFN-γ, CD4+ IFN-γ, DN IFN-γ], and Group 2 [DP IL-4]. Repeated stress did not significantly impact the aggregate Groups (Figure 4C(ii) upper left panel; stress × group interaction $p = 0.2259$, $F(2,23) = 1.559$; main effect of stress $p = 0.237$, $F(1,16) = 1.510$, two-way RM-ANOVA), although the Group 1 values were correlated with the number

of attacks ($p = 0.0446$ after correction; Figure 4C(ii) lower left panel). The ratios of the 3 groups were calculated to determine if stress shifted the balance between groups. Repeated stress shifted the balance between groups (Figure 4C(ii) upper right panel; main effect of stress $p = 0.0143$, F(2,32) = 4.868, two-way RM-ANOVA), such that Group 1 (predominantly IL-4 cells) increased relative to Group 3 cells (predominantly IFN-γ cells ($p < 0.05$ after Bonferroni corrections). This Group 1:Group 3 balance was significantly correlated with the number of attacks (Figure 4C(ii) lower right panel, $p < 0.05$ after Bonferroni corrections).

Because the overall Th1 cell and overall Th2 cell populations may be important, even though they did not cluster together, this analysis was repeated with Th1 cells all clustered together and Th2 cells all clustered together. However, neither the aggregate Th1 cells, aggregate Th2 cells, nor their ratio reached a significant effect of stress (stress × group interaction $p = 0.1270$, F(1,16) = 2.591, main effect of stress $p = 0.1544$, F(1,16) = 2.235, two-way RM-ANOVA) although a clear trend was observed, and these values were not correlated with number of attacks ($p > 0.05$ for all correlations). These data suggest that when specific Th1 and Th2 clusters of cells are considered, repeated stress can shift the balance of these cells towards Th2 profiles.

3.3. RSDS shifts peripheral circulatory cytokines towards a pro-inflammatory profile

The intracellular cytokine profile is important. However, not all T-cells are positive for IL-4 or IFN-γ. This is evidenced by increased CD4+ and CD8+ IL-4 cells after stress, but a decreased overall CD4+ cells, and no significant effect in overall CD8+ cells after stress. One possible interpretation is that a difference in cytokine release from these populations can lead to a relative shift in IL-4/IFN-γ-positive cells. A shift in the balance between Th1/Th2 T-cells would be expected to produce a shift in the peripheral cytokine profile. This was tested with ELISA measures from serum and quantified as fold-changes compared to the respective controls. For initial analysis, cytokines were characterized as pro-inflammatory or anti-inflammatory cytokines based on the known predominant inflammatory nature of the cytokines; we used a commercially available ELISArray kit (method) to screen twelve cytokines (nine pro-inflammatory and three anti-inflammatory) that was available for such cytokine screening purpose.

3.3.1. Pro-inflammatory cytokine profile—The fold-change of cytokines was measured. After corrections, only the pro-inflammatory cytokines **IL-1β** ($p < 0.0001$) and **IL-6** ($p < 0.01$) were significantly increased (Bonferroni's multiple comparisons tests; Figure 5A left panel). There was no significant correlation between any of the cytokines and the number of attacks (all $p > 0.05$; data not shown). **IL-1β** (Control: N = 12 rats, 1.00 ± 0.209; RSDS: N = 13 rats, 4.210 ± 1.242; t = 2.449, df = 23, $p = 0.02$, unpaired t-test), **IL-6** (Control: N = 12 rats, 1.00 ± 0.106; RSDS: N = 13 rats, 3.328 ± 0.758; U = 21.50, $p = 0.001$, Mann-Whitney U test), **IL-12** (Control: N = 14 rats, 0.9999 ± 0.293; RSDS: N = 14 rats, 1.710 ± 0.509; U = 53, $p = 0.03$, Mann-Whitney U test), **TNF-α** (Control: N = 13 rats, 1.00 ± 0.087; RSDS: N = 14 rats, 1.548 ± 0.224; t = 2.207, df =25, $p = 0.03$, unpaired t-test) and **GM-CSF** (Control: N = 14 rats, 1.00 ± 0.217; RSDS: N = 14 rats, 1.755 ± 0.337; t = 1.883, df = 26, $p = 0.07$, unpaired t-test).

There was a trend (0.10 > p > 0.05) towards an increase in the fold-change of serum pro-inflammatory cytokines **IL-1α** (Control: N = 12 rats, 1.00 ± 0.137; RSDS: N = 13 rats, 1.715 ± 1.317; U = 47, p = 0.09, Mann-Whitney U test), and **IL-2** (Control: N = 14 rats, 1.00 ± 0.222; RSDS: N = 14 rats, 1.953 ± 0.520; t = 1.684, df = 26, p = 0.10, unpaired t-test).

The remaining measured cytokines were not significantly different in RSDS compared to control, and did not show a trend toward significantly different fold-change, including **IFN-γ** (Control: N = 14 rats, 1.000 ± 0.396; RSDS: N = 14 rats, 0.908 ± 0.209; U = 81, p = 0.447, Mann-Whitney U test) and **RANTES** (Control: N = 14 rats, 1.000 ± 0.277; RSDS: N = 11 rats, 0.802 ± 0.111; U = 60, p = 0.365, Mann-Whitney U test).

3.3.2.   Anti-inflammatory cytokine profile—Traditional anti-inflammatory cytokines were measured in a similar manner. There was no significant difference between RSDS and control in the fold-changes of any of the serum anti-inflammatory cytokines measured (Figure 5A right panel). This includes **IL-4** (Control: N = 14 rats, 1.000 ± 0.308; RSDS: N = 14 rats, 1.263 ± 0.366; U = 82, p = 0.475, Mann-Whitney U test), **IL-10** (Control: N = 13 rats, 1.000 ± 0.268; RSDS: N = 14 rats, 1.171 ± 0.293; U = 64, p = 0.197, Mann-Whitney U test), and **IL-13** (Control: N = 14 rats, 1.000 ± 0.335; RSDS: N = 14 rats, 1.095 ± 0.280; U = 68, p = 0.178, Mann-Whitney U test).

3.3.3.   Balance between clusters of cytokines—Cytokines fell into 3 groups based on PCA and hierarchical analysis (Figure 5B): Group 1 [IL-1β, IL-2, IFN-γ, RANTES], Group 2 [IL-1α, IL-6, TNFα, GM-CSF], and Group 3 [IL-4, IL-10, IL-12, IL-13]. The effect of stress on the aggregated groups was tested (Figure 5C; main effect of stress p = 0.0486, F(1,26) = 4.283, two-way RM-ANOVA). Repeated stress increased Group 2 cytokines (p < 0.05 post hoc Bonferroni). The balance between these groups was measured as the ratios between each combination of groups, and the effect of stress was tested (main effect of stress p = 0.0330, F(1,26) = 5.074), with a shift towards both greater Group 1 and Group 2 cytokines relative to Group 3 (Figure 5C upper left panel; Group 1:Group 3 ratio and Group 2:Group 3 ratio, p < 0.05 post hoc Bonferroni). In addition, the ratios of all these groups were correlated with the number of attacks (Figure 5C lower panel; p < 0.05 after post hoc Bonferroni corrections). This indicates that two separate groups of cytokines, both of which include traditional pro-inflammatory cytokines, are differentially associated with a shift in the balance of cytokines after stress, specifically relative to a third group that includes traditional anti-inflammatory cytokines.

3.4.   RSDS increases activated microglia in the BLA

Our results suggest that RSDS causes a shift of the peripheral cytokines and T-cell population, as well as changes in anxiety. The BLA is a key region involved in anxiety, so we next examined the effects of stress on microglia, the primary inflammatory cells in the brain. The number of microglia cells can be indicative of immune activation. RSDS caused a trend towards an increase in the number of Iba-1-positive microglia in the BLA, compared to control (Figure 6A left panel). When comparing across BLA nuclei, the microglia number was significantly increased in the BA but was unaffected in the LAT in the RSDS group

compared to the control (Figure 6A right panel). There was no significant correlation between the number of attacks encountered by the defeated rats and the microglia counts (all $p > 0.05$, data not shown).

Microglia were also characterized into three morphological categories depending on the stages of their activation (Methods). RSDS shifted the proportion of microglia in these three morphological categories (Figure 6D upper panel; stress × microglia group interaction, $p = 0.042$, $F(6,40) = 2.433$, two-way RM-ANOVA). The resting group I (ramified) microglia count was significantly reduced by stress in BA and the LAT nuclei ($p < 0.05$, post hoc Bonferroni multiple comparisons test). There was no significant correlation between the total number of attacks encountered by the defeated rats and the counts of the microglia types (all $p > 0.05$, data not shown). In keeping with the goal of this study to determine whether a shift in the balance between immune states may be important, the ratio of resting group I to activated group III microglia was measured in control and stress groups. Stress caused a significant shift towards group III microglia (Figure 6D lower panel). There was no significant correlation between the total number of attacks encountered by the defeated rats and these ratios (all $p > 0.05$, data not shown).

To further measure microglia in the BLA, cells were immunostained for Iba-1 and CD68, with double labeled cells considered activated microglia, separated as ramified or minimally ramified cells. Stress did not significantly impact the percent of co-labeled cells in the LAT (Figure 6E, right), nor in the BA (Figure 6E, left). To examine whether there was a shift between ramified and minimally ramified microglia, their ratio was compared. Stress significantly shifted the ratio towards less ramified microglia in the BA (Figure 6F, left), with no consistent effect in the LAT (Figure 6F, right).

3.5. RSDS increases BLA neuronal firing

Our results found that RSDS increased anxiety behaviors, which could be driven by BLA neuronal hyperactivity. In addition, glial activity can be associated with neuronal activity, and we found that RSDS increased glial activity. While previous studies have tested the effects of other stressors on the *in vivo* firing of BLA neurons, the effects of RSDS had not yet been examined. The firing of single neurons was recorded from BA and LAT nuclei of anesthetized rats (Figure 7A, B, C). RSDS increased the firing rate of neurons from the BA (Figure 7A, B) and the LAT (Figure 7A, B).

In order to examine any association between the stress and the effect on BLA neuronal activity, we tested for correlation between the total number of physical attacks by the aggressor on the experimental rats and the average firing rate of BA and LAT nuclei from the same rats. Our data (Figure 7D) showed a significant positive correlation between the number of attacks and the firing rate in both the BA (Figure 7D left panel; linear fit, $R^2 = 0.943$, $F(1,4) = 66.61$, $p = 0.001$) and the LAT (Figure 7D right panel; linear fit, $R^2 = 0.896$, $F(1,4) = 34.78$, $p = 0.004$) nuclei. This result suggests that severity of repeated social stress was associated with increased neuronal firing of BA and LAT nuclei.

3.6 Minocycline reduces effects of RSDS on BLA neuronal firing

To link activation of microglia with effects of stress on BLA neuron firing, minocycline was administered prior to each social defeat stress. This design allows testing of whether microglia activation is important for establishment of the effects of stress on BLA neuron firing. Minocycline dampened the effects of repeated stress on BA neuron firing (main effect p = 0.039, F(1,127) = 4.35, two-way ANOVA; control-saline n = 15 neurons / 7 rats, control-minocycline n = 16 neurons / 5 rats, stress-saline n = 49 neurons / 11 rats, stress-minocycline n = 51 neurons / 7 rats), but did not exert consistent effects on LAT neuron firing (main effect p = 0.162, F(1,81) = 1.99; control-saline n = 14 neurons, control-minocycline n = 18 neurons, stress-saline n = 48 neurons, stress-minocycline n = 8 neurons). This could be due in part to the relatively smaller number of active neurons recorded from the LAT of stress rats after minocycline, despite substantial efforts. This might indicate that minocycline greatly shifted the activity of LAT neurons to below firing threshold levels in this condition.

4.   Discussion

In this study, we examined the effects of repeated social defeat stress on immune system parameters in rats. Although earlier studies have shown an association between altered immune status and stress and stress-associated disorders, few studies provide a holistic assessment of the effects of repeated stress on the immune system, as performed here. The underlying rationale was that better understanding of changes can be achieved by clustering immune parameters based on how they co-vary, in contrast to potentially inaccurate grouping based on pro- or anti-inflammatory actions. Therefore, one goal of this study was to test whether there are groups of peripheral immune parameters that co-vary together as a result of stress, and whether the balance between these groups is shifted by stress. Evidence also suggests that actions in the amygdala are an important mediator of the effects of stress on anxiety. Therefore, a second goal of this study was to link immune imbalance to anxiety behaviors and an immune-related change in the amygdala. This was achieved by testing whether stress produced a shift in microglia balance in the BLA, and if microglia interference was sufficient to block the effects of stress on BLA neuron activity.

Our data demonstrate that repeated stress increases anxiety-like behavior and increases the early precursor dual negative T-cells in circulation while decreasing the dual positive and mature CD4+ T-cells. This suggests that social stress affects the differentiation and proliferation of immune cells in the periphery. Progenitor T-cells from the bone-marrow are carried through the blood to the thymus, where they pass through the dual negative stages to the dual positive stage by expressing T-cell receptors (TCR) (Germain, 2002; Starr et al., 2003). The survival of the dual positive cells is controlled by the appropriate TCR signaling within the cells, which results in the negative selection of the cells to differentiate into CD4+ or CD8+ T-cells. Thus passing the negative selection check-point is crucial in the ultimate commitment of the cells to develop into the CD4+ or CD8+ T-cells (Ioannidis et al., 2001; He et al., 2010; Koch and Radte, 2011). Our current findings that RSDS causes an increase in the dual negative and decrease in the dual positive and CD4+ T-cells might indicate a probable effect of social stress on this T-cell selection process, most likely affecting the

negative selection check-point. This restriction on immune flexibility is possibly worsened by the decrease of Treg cells, as loss of Treg cells can lead to inability to hold immune responses in check after their initiation. A decrease in Treg cells may contribute to shifts of immune function observed in the current study. Consistent with this, a decrease in Treg cells is associated with development of depressive-like behavior and pro-inflammatory state (Kim et al., 2012; Hong et al., 2013; Li et al., 2016). Targeting signaling pathways that regulate differentiation of T-cells, or specific T-cells, may provide an initial step towards preventing the effects of stress on immune function.

We found that chronic stress increases the traditional pro-inflammatory (Th1) response in circulation, as evidenced by increase in pro-inflammatory cytokine levels in serum (Figure 5A), whereas intracellular positivity for type-2 (Th2 and Tc2) cytokines are significantly increased in the CD4+ and CD8+ T-cells (Figure 4). There may be several reasons for this. Th1 cytokines are secreted from the cells to the circulation, thereby increasing the serum levels of these cytokines, but leading to a reduction in their intracellular content and a relative increase in the proportion of cells with Th2 (or Tc2) cytokines. In addition, T-cells are present in peripheral lymphoid regions, such as spleen, lymph nodes and mucosa-associated lymphoid tissue which may have different intracellular content of the cytokines than circulating T-cells. An earlier study had also shown reduction of CD4+ T-cells and intra-lymphocyte pro-inflammatory cytokine mRNAs (TNF-α and IFN-γ) within lymph nodes of mice exposed to chronic restraint stress compared to controls (Frick et al., 2009). Our present study focused on the count and intracellular cytokine profile of only the circulatory T-cell population.

Although exposure to social defeat is associated with increased myeloid-derived immune cells (e.g. granulocytes, monocytes) in circulation, there are several reasons why we chose to focus on the effect of RSDS on the peripheral T-cells: (i) Cell-mediated immune response is known to be affected in depression (Maes, 2011; Maes et al., 2011). Since T-cells are an important source of cytokine secretion (Huse et al., 2006; Bhandage et al., 2018) and an important component of the immune response overall, we focused on the T-cells. (ii) Stress causes cognitive impairment (Yuen et al., 2012; Shansky and Lipps, 2013). T-cell deficiency also leads to cognitive dysfunctions (Kipnis et al., 2004). Adaptive immunity conferred by T-cells is known to affect the cognitive and learning behavioral responses (Brynskikh et al., 2008; Radjavi et al., 2014). We thus hypothesized that RSDS used in our study might affect T-cells. (iii) T-cells patrol the CNS borders in the meningeal spaces (Louveau et al., 2015; Filiano et al., 2017), and are important in maintaining the homeostasis of CNS functions (Ellwardt et al., 2016). Thus T-cells can affect neuro-immune connection during inflammatory states. (iv) T-cells from the periphery can modulate CNS activity in neuro-immune conditions (Arima et al., 2012; Sabharwal et al., 2014), and therefore peripheral T-cells might be a key player in mediating the neuro-immune effect of RSDS. (v) T-cells may be capable of trafficking to the brain from the periphery, both in health and during diseased state (Engelhardt and Ransohoff, 2005; Schmitt et al., 2012; Strazielle et al., 2016; Brown and Sawchenko, 2007), and these cells can trigger microglia activation. Identifying changes in T-cell population in stress might help in a novel understanding of the avenue for developing potential cell-targeted therapy by targeting the developmental and maturation stages of peripheral T-cells in the management of anxiety and depressive disorders.

A unique finding in this study is that unbiased grouping of cytokines produces a different picture of the effects of stress. The grouping of cytokines was not based on *a priori* assumption of pro- or anti-inflammatory effect, but instead based on whether the cytokines change together. This lead to the observation that stress effects on groups of cytokines did not match traditional pro- or anti-inflammatory boundaries. The primary groups can include traditional pro-inflammatory and anti-inflammatory cytokines (Group 1: Il-1b, IL-2, IFN-g, RANTES; Group 2: IL-1a, IL-6, TNF-a, GM-CSF; Group 3: IL-4, IL-10, IL-12, IL-13). The relative amounts of these cytokines was impacted by stress. This suggests that broad anti-inflammatory approaches can be refined to, instead, target a handful of cytokines to diminish the effects of stress.

Earlier studies have shown that recruitment of myeloid cells from the periphery to the brain is required for the development of anxiety in mice after RSDS (Wohleb et al., 2013), monocyte trafficking from the spleen to the brain contributes to the re-establishment of anxiety in stress-sensitized mice (Wohleb et al., 2014), and microglia in the brain are derived from erythro-myeloid precursor cells (Gomez Perdiguero et al., 2015; Herz et al., 2017). Myeloid cells affect the proliferation and function of T-cells (Nagaraj et al., 2010; Stroncek et al., 2016; Van de Velde et al., 2017), and T-cells affect myeloid cell differentiation (Paschall et al., 2015). However, we acknowledge that T-cells are only one component that may be important in the effects of stress. Furthermore, how the change in T-cells relates to the observed changes in cytokines and BLA physiology, and how the CNS changes may then impact peripheral immune function, was not examined and remain important questions. Stress hormones such as catecholamines and glucocorticoids acutely reduce Th1 and increase Th2 responses (Elenkov and Chrousos, 2002; Calcagni and Elenkov, 2006). Glucocorticoids are increased after RSDS (Niraula et al., 2018), and this prolonged elevation can lead to decreased immune sensitivity to glucocorticoids (Avitsur et al., 2001; Stark et al, 2002). Thus it is possible that impaired regulation by glucocorticoids or enhanced CNS-driven sympathetic output may contribute to elevated serum cytokine levels observed after repeated social stress.

Chronic stress causes behavioral and cognitive changes (Lapiz-Bluhm et al., 2009), in part via neuroimmune changes (Girotti et al., 2011; Kang et al., 2012; Ota et al., 2014). Although the peripheral signal that ultimately leads to BLA neuronal hyperactivity is not clear, a parsimonious explanation would be that it can occur via immune changes in the BLA. Within the brain, proliferation and activation of microglia reflects an immunoresponse and further propogates immune changes. Activation of microglia can be observed as retraction of processes towards their cell bodies (Brown and Vilalta, 2015), increased expression of Iba-1, and expression and secretion of cytokines, namely IL-1, IL-6, TNF-α and IFN-γ. Thus, the decrease in the number of group I (ramified) and increase in the number of group III (ameboid) microglia seen in the RSDS group of our current study suggests that the repeated stress activates microglia in the BA (Figure 6E). Further, there was a shift in the balance between group III (ameboid) microglia and group I microglia in both the BA and LAT (Figure 6E), suggesting increased microglia activation. Similar to alterations in ameboid states, RSDS increased the number of Iba-1 positive microglia in the BA nuclei (Figure 6), with a trend towards increase in the LAT. These results provide two morphological measures of microglia activation within the BLA to suggest repeated social stress increases neural

immune states. These results could be due to 1) recruitment of new microglia to the BLA, 2) elevated expression of Iba-1 so that more cells are above the detection limit, or 3) rapid proliferation of microglia. To further examine the activation states of microglia beyond morphological analysis, we also measured CD68 expression, as this is a reliable marker for microglia activation. CD68 marks microglia phagocytosis, and alterations of this protein have been seen with a compromised immune system in the BLA (Acharjee et al., 2018). This further supported a shift towards microglia activation in the BA, although the results were not as robust as with Iba-1 staining alone.

Activated microglia secrete pro-inflammatory cytokines that propagate immune signals within the brain, that can then participate in the physiological and behavioral responses to neuroimmune activation (Dantzer, 2001; Dantzer et al., 2008; Norden et al., 2016). Microglial activation impacts the release of neuromodulators, alters neuronal morphology and impacts synaptic function (Wu et al., 2015; Wohleb et al., 2016). Phagocytic actions of microglia physically remodel synaptic networks (Kettenmann et al., 2013). Activated microglia can potentially increase neuronal excitability, disrupt neural network and cause neuronal death (Werneburg et al., 2017; Acharjee et al., 2018). Earlier studies have shown that activated microglia, by releasing pro-inflammatory cytokines or Brain-Derived Neurotrophic Factor (BDNF), increase neuronal excitability (Klapal et al., 2016) or suppress fast GABAergic inhibition of neurons (Rivera et al., 2002; Ferrini and De Koninck, 2013). These microglial actions might contribute to the effects of stress on BLA neuronal firing observed here.

There are several signals that may produce microglial activation. Stress induces elevation of catecholamine levels in the brain that can shift microglia towards an activated state (Blandino et al., 2006; Walker et al., 2013), and peripheral immune changes can produce CNS immune changes (see below). Repeated social defeat in mice has been shown to increase the IL-1β mRNA within the microglia along with activation of the β-adrenoceptor and IL-1β receptor on microglia (Wohleb et al., 2011). We found that suppression of microglia activation proximal to the social defeat stress was able to mitigate the effects of stress on BLA neuron firing. This provides a strong link between the effects of stress on microglia and the effects of stress on BLA neurons. We acknowledge that although we have not explored the different factors regulating the microglial activation, their functions, and the changes in cytokine genes in the BLA after RSDS, future studies aiming to find these effects after RSDS will be very valuable.

Earlier studies have found that peripheral immune and inflammatory activation affects amygdala activity. One study involving human participants found that *Escherichia coli* endotoxin injection heightened amygdala activity in response to socially threatening images (fear faces), which was associated with increased feelings of social withdrawal (Inagaki et al., 2012). Meta-analysis further implicated the amygdala as part of a network of neural structures activated by acute or chronic inflammation in humans (Kraynak et al, 2018). LPS injection also increases BLA neuronal activity in rodents evidenced by c-Fos immunoreactivity 2 hr post-treatment (Engler et al., 2011) and increases expression of IL-1β, IL-6, and TNF-α mRNA levels that is suggestive of *de novo* synthesis of these cytokines in the amygdala following peripheral immune activation (Engler et al., 2011).

Acute peripheral immune activation by IL-1β causes an increase of BLA neuronal activity and anxiety as well (Munshi and Rosenkranz, 2018). The findings from our present study may help link effects of acute inflammation with effects of longer-lasting stress-induced peripheral immune activation. We observed a significant increase in the BLA neuronal firing after the stress that correlated positively with the severity of the stress (Figure 7D), and was mitigated by blockade of microglia activation.

While these results collectively suggest that microglia play an important role in establishment of the effects of stress on BLA neurons, this does not rule out the possibility of other direct or indirect effects of cytokines on BLA neurons. There are several ways in which this may occur, such as active transport of cytokines from the periphery to the brain (Banks, 2005), diffusion of cytokines from the periphery to the brain via areas devoid of the blood-brain barrier (Stitt, 1990), and volume transmission of the cytokines via brain parenchyma to the BLA (Banks et al., 1995; Dantzer et al., 2000; Konsman et al., 2002; Felger and Lotrich, 2013). In addition, activation of peripheral vagal afferents can increase cytokines in the brain (Maier et al., 1998). Once in the brain, there are also several ways in which cytokines can impact the activity of neurons, such as by facilitating the release of neuromodulators from glia and endothelial cells in the brain, or by directly influencing synaptic transmission and neuronal excitability via neuronal receptors (Viviani et al., 2007; Vezzani et al., 2011; Gadek-Michalska et al., 2013; Marin and Kipnis, 2013; Vezzani and Viviani, 2015). Examples include direct neuronal effects of IL-1β on GABA$_A$ receptor function (Miller et al., 1991), depression of voltage-gated calcium channel currents (Plata-Salaman and French-Mullen, 1992), and NMDA receptor mediated increase in the intracellular calcium (Viviani et al., 2003). Elevated IL-6 can cause increased excitatory synaptic transmission in the hippocampus (Nelson et al., 2012) and TNF-α can enhance excitatory AMPA-mediated input (Ogoshi et al., 2005) while decreasing the GABA-mediated inhibitory synaptic strength (Stellwagen et al., 2005). These are potential direct means by which the immune system can promote effects observed here. However, little is known about effects of cytokines in the amygdala. IL-1β can globally increase electroencephalographic activity in the amygdala (Engler et al., 2011), and impact spontaneous action potential-independent transmission of central amygdala GABAergic neurons via both pre- and post-synaptic mechanisms (Bajo et al., 2015). TNF-α has also been shown to increase firing rate and GABA release in rat central amygdala neurons in vitro (Knapp et al., 2011). Even less is known about effects of cytokines on the excitability of BLA neurons. IL-1β can decrease the excitability of BLA neurons *in vitro* (Yu and Shinnick-Gallagher, 1994). Recently, we have shown that peripherally administered IL-1β increases the spontaneous neuronal firing of BLA neurons *in vivo* (Munshi and Rosenkranz, 2018), an effect reminiscent of the effects of stress observed here. Thus, there is precedent for effects of immune activation on BLA neuronal activity, and this could account for the effects of repeated stress on BLA neuronal activity.

We also acknowledge the limitation of using anesthesia for the brain collection for immunohistochemistry, BLA electrophysiology, and blood collection for flow cytometry experiments. Although we have used the same anesthetic in the respective control groups for the experiments, the limitations associated with anesthesia cannot be overlooked. Urethane was used in electrophysiology experiments because of its potent action in maintaining a

deep anesthesia state over the course of hours, allowing stable recordings and sampling within the BLA. Urethane was also used for blood collection for the FACS experiments to keep conditions similar to the electrophysiology experiments.

5. Conclusions

Chronic stress, which is an important factor contributing to the development of depression, has significant effects on the immune system parameters. Here we examined the effects of chronic stress on the circulating immune parameters using the resident-intruder model of repeated social defeat stress (RSDS) in adult male rats. We have also examined the effect of the stress on the resident immune cells of the amygdala (BLA), the microglia, as well as the BLA neuronal firing *in vivo*. The findings from this study give a more holistic picture of the changes occurring in the peripheral immune system during RSDS. The salient finding of shifts in coordinated groups of peripheral cytokines clarifies and reorganizes the peripheral effects, and suggests targeting of subsets of cytokines instead of broad immunosuppression, while parallel shifts in the BLA link immune changes with neuronal activity during repeated stress. These coordinated changes may explain the co-morbidity of different inflammatory conditions associated with chronic stress and psychological disorders triggered by chronic stress.

ACKNOWLEDGEMENTS

ABBREVIATIONS

BA	Basal nucleus of BLA
BLA	Basolateral amygdala
DN	Dual negative
DP	Dual positive
ELISA	Enzyme-linked immunosorbent assay
EPM	Elevated plus maze
FACS	Fluorescence-activated cell sorting
ICS	Intracellular cytokine staining

| **LAT** | Lateral nucleus of BLA |
| **RSDS** | Repeated social defeat stress |

References

Acharjee S, Verbeek M, Gomez CD, Bisht K, Lee B, Benoit L, Sharkey KA, Benediktsson A, Tremblay ME, Pittman QJ (2018) Reduced Microglial Activity and Enhanced Glutamate Transmission in the Basolateral Amygdala in Early CNS Autoimmunity. J Neurosci 38: 9019–9033. [PubMed: 30185466]

Ahmad SF, Zoheir KM, Ansari MA, Korashy HM, Bakheet SA, Ashour AE, Attia SM (2015) Stimulation of the histamine 4 receptor with 4-methylhistamine modulates the effects of chronic stress on the Th1/Th2 cytokine balance. Immunobiology 220:341–349. [PubMed: 25457414]

Anisman H, Merali Z (2002) Cytokines, stress, and depressive illness. Brain Behav Immun 16:513–524. [PubMed: 12401465]

Arima Y, Harada M, Kamimura D, Park JH, Kawano F, Yull FE, Kawamoto T, Iwakura Y, Betz UA, Marquez G, Blackwell TS, Ohira Y, Hirano T, Murakami M (2012) Regional neural activation defines a gateway for autoreactive T cells to cross the blood-brain barrier. Cell (United States) 148:447–457.

Avitsur R, Stark JL, Sheridan JF (2001) Social stress induces glucocorticoid resistance in subordinate animals. Horm Behav 39: 247–257. [PubMed: 11374910]

Azzinnari D, Sigrist H, Staehli S, Palme R, Hildebrandt T, Leparc G, Hengerer B, Seifritz E, Pryce CR (2014) Mouse social stress induces increased fear conditioning, helplessness and fatigue to physical challenge together with markers of altered immune and dopamine function. Neuropharmacology 85:328–341. [PubMed: 24907589]

Bajo M, Varodayan FP, Madamba SG, Robert AJ, Casal LM, Oleata CS, Siggins GR, Roberto M (2015) IL-1 interacts with ethanol effects on GABAergic transmission in the mouse central amygdala. Front Pharmacol (Switzerland) 6:49.

Banks WA (2005) Blood-brain barrier transport of cytokines: A mechanism for neuropathology. Curr Pharm Des (United Arab Emirates) 11:973–984.

Banks WA, Kastin AJ, Broadwell RD (1995) Passage of cytokines across the blood-brain barrier. Neuroimmunomodulation (Switzerland) 2:241–248.

Bartolomucci A, Leopardi R (2009) Stress and depression: Preclinical research and clinical implications. PLoS One 4:e4265. [PubMed: 19180237]

Bartolomucci A, Palanza P, Gaspani L, Limiroli E, Panerai AE, Ceresini G, Poli MD, Parmigiani S (2001) Social status in mice: behavioral, endocrine and immune changes are context dependent. Physiol Behav 73:401–410. [PubMed: 11438368]

Berner B, Akca D, Jung T, Muller GA, Reuss-Borst MA (2000) Analysis of Th1 and Th2 cytokines expressing CD4+ and CD8+ T cells in rheumatoid arthritis by flow cytometry. J Rheumatol 27:1128–1135. [PubMed: 10813277]

Berton O, McClung CA, Dileone RJ, Krishnan V, Renthal W, Russo SJ, Graham D, Tsankova NM, Bolanos CA, Rios M, Monteggia LM, Self DW, Nestler EJ (2006) Essential role of BDNF in the mesolimbic dopamine pathway in social defeat stress. Science 311:864–868. [PubMed: 16469931]

Beynon SB, Walker FR (2012) Microglial activation in the injured and healthy brain: What are we really talking about? practical and theoretical issues associated with the measurement of changes in microglial morphology. Neuroscience (United States) 225:162–171.

Bhandage AK, Jin Z, Korol SV, Shen Q, Pei Y, Deng Q, Espes D, Carlsson PO, Kamali-Moghaddam M, Birnir B (2018) GABA regulates release of inflammatory cytokines from peripheral blood mononuclear cells and CD4(+) T cells and is immunosuppressive in type 1 diabetes. Ebiomedicine (Netherlands) 30:283–294.

Blandino P Jr, Barnum CJ, Deak T (2006) The involvement of norepinephrine and microglia in hypothalamic and splenic IL-1beta responses to stress. J Neuroimmunol (Netherlands) 173:87–95.

Bollinger JL, Collins KE, Patel R, Wellman CL (2017) Behavioral stress alters corticolimbic microglia in sex- and brain region-specific manner. PLoS One 12:e0187631. [PubMed: 29194444]

Boschen KE, Hamilton GF, Delorme JE, Klintsova AY (2014) Activity and social behavior in a complex environment in ratsneonatally exposed to alcohol. Alcohol 48: 533–541 [PubMed: 25150044]

Bowers SL, Bilbo SD, Dhabhar FS, Nelson RJ (2008) Stressor-specific alterations in corticosterone and immune responses in mice. Brain Behav Immun 22:105–113 [PubMed: 17890050]

Breen MS, Tylee DS, Maihofer AX, Neylan TC, Mehta D, Binder EB, Chandler SD, Hess JL, Kremen WS, Risbrough VB, Woelk CH, Baker DG, Nievergelt CM, Tsuang MT, Buxbaum JD, Glatt SJ (2018) PTSD Blood Transcriptome Mega-Analysis: Shared Inflammatory Pathways across Biological Sex and Modes of Trauma. Neuropsychopharmacology 43:469–481 [PubMed: 28925389]

Brown DA, Sawchenko PE (2007) Time course and distribution of inflammatory and neurodegenerative events suggest structural bases for the pathogenesis of experimental autoimmune encephalomyelitis. J Comp Neurol (United States) 502:236–260.

Brown GC, Vilalta A (2015) How microglia kill neurons. Brain Res 1628 (Pt B): 288–297 [PubMed: 26341532]

Brynskikh A, Warren T, Zhu J, Kipnis J (2008) Adaptive immunity affects learning behavior in mice. Brain Behav Immun (Netherlands) 22:861–869.

Budiu RA, Vlad AM, Nazario L, Bathula C, Cooper KL, Edmed J, Thaker PH, Urban J, Kalinski P, Lee AV, Elishaev EL, Conrads TP, Flint MS (2017). Restraint and Social Isolation Stressors Differentially Regulate Adaptive Immunity and Tumor Angiogenesis in a Breast Cancer Mouse Model. Cancer Clin Oncol 6:12–24 [PubMed: 28603578]

Calcagni E, Elenkov I (2006) Stress system activity, innate and T helper cytokines, and susceptibility to immune-related diseases. Ann N Y Acad Sci 1069:62–76. [PubMed: 16855135]

Caserta MT, O'Connor TG, Wyman PA, Wang H, Moynihan J, Cross W, Tu X, Jin X (2008) The associations between psychosocial stress and the frequency of illness, and innate and adaptive immune function in children. Brain Behav Immun 22:933–940 [PubMed: 18308510]

Chida Y, Sudo N, Kubo C (2005) Social isolation stress exacerbates autoimmune disease in MRL/lpr mice. J Neuroimmunol 158:138–144. [PubMed: 15589047]

Cole SW, Hawkley LC, Arevalo JM, Cacioppo JT (2011) Transcript origin analysis identifies antigen-presenting cells as primary targets of socially regulated gene expression in leukocytes. Proc Natl Acad Sci 108, 3080–3085. doi: 10.1073/pnas.1014218108Corthay A (2009) How do regulatory T cells work? Scand J Immunol 70:326–336. [PubMed: 21300872]

Dantzer R (2001) Cytokine-induced sickness behavior: Mechanisms and implications. Ann N Y Acad Sci 933:222–234. [PubMed: 12000023]

Dantzer R, Konsman JP, Bluthe RM, Kelley KW (2000) Neural and humoral pathways of communication from the immune system to the brain: parallel or convergent? Auton Neurosci 85:60–65 [PubMed: 11189027]

Dantzer R, O'Connor JC, Freund GG, Johnson RW, Kelley KW (2008) From inflammation to sickness and depression: When the immune system subjugates the brain. Nat Rev Neurosci (England) 9:46–56.

Deak T, Bellamy C, D'Agostino LG (2003) Exposure to forced swim stress does not alter central production of IL-1. Brain Res 972:53–63 [PubMed: 12711078]

Deak T, Bordner KA, McElderry NK, Barnum CJ, Blandino P Jr, Deak MM, Tammariello SP (2005) Stress-induced increases in hypothalamic IL-1: a systematic analysis of multiple stressor paradigms. Brain Res Bull 64:541–556 [PubMed: 15639551]

del Rio-Hortega P (1932) Microglia In: Cytology and Cellular Pathology of the Nervous System, edited by Penfield W New York: Hoeber, p. 482–1924–534.

Dunphy-Doherty F, O'Mahony SM, Peterson VL, O'Sullivan O, Crispie F, Cotter PD, Wigmore P, King MV, Cryan JF, Fone KCF (2018) Post-weaning social isolation of rats leads to long-term disruption of the gut microbiota-immune-brain axis. Brain Behav Immun 68:261–273 [PubMed: 29104061]

Eddy P, Heckenberg R, Wertheim EH, Kent S, Wright BJ (2016) A systematic review and meta-analysis of the effort-reward imbalance model of workplace stress with indicators of immune function. J Psychosom Res 91:1–8 [PubMed: 27894456]

Elenkov IJ, Chrousos GP (2002) Stress hormones, pro-inflammatory and antiinflammatory cytokines, and autoimmunity. Ann N Y Acad Sci 966:290–303. [PubMed: 12114286]

Ellwardt E, Walsh JT, Kipnis J, Zipp F (2016) Understanding the role of T cells in CNS homeostasis. Trends Immunol (England) 37:154–165.

Engelhardt B, Ransohoff RM (2005) The ins and outs of T-lymphocyte trafficking to the CNS: Anatomical sites and molecular mechanisms. Trends Immunol (England) 26:485–495.

Engler H, Doenlen R, Engler A, Riether C, Prager G, Niemi MB, Pacheco-Lopez G, Krugel U, Schedlowski M (2011) Acute amygdaloid response to systemic inflammation. Brain Behav Immun 25:1384–1392. [PubMed: 21521653]

Felger JC, Lotrich FE (2013) Inflammatory cytokines in depression: neurobiological mechanisms and therapeutic implications. Neuroscience 246:199–229. [PubMed: 23644052]

Ferrini F, De Koninck Y (2013) Microglia control neuronal network excitability via BDNF signalling. Neural Plast (United States) 2013:429815.

File SE, Hyde JR (1978) Can social interaction be used to measure anxiety? Br J Pharmacol 62:19–24 [PubMed: 563752]

Filiano AJ, Gadani SP, Kipnis J (2017) How and why do T cells and their derived cytokines affect the injured and healthy brain? Nat Rev Neurosci (England) 18:375–384.

Frick LR, Arcos ML, Rapanelli M, Zappia MP, Brocco M, Mongini C, Genaro AM, Cremaschi GA (2009) Chronic restraint stress impairs T-cell immunity and promotes tumor progression in mice. Stress (England) 12:134–143.

Gadek-Michalska A, Tadeusz J, Rachwalska P, Bugajski J (2013) Cytokines, prostaglandins and nitric oxide in the regulation of stress-response systems. Pharmacol Rep (Poland) 65:1655–1662.

Gerritsen W, Heijnen CJ, Wiegant VM, Bermond B, Frijda NH (1996) Experimental social fear: immunological, hormonal, and autonomic concomitants. Psychosom Med. 58:273–286 [PubMed: 8771627]

Ginhoux F, Greter M, Leboeuf M, Nandi S, See P, Gokhan S, Mehler MF, Conway SJ, Ng LG, Stanley ER, Samokhvalov IM, Merad M (2010) Fate mapping analysis reveals that adult microglia derive from primitive macrophages. Science 330:841–845. [PubMed: 20966214]

Ginhoux F, Lim S, Hoeffel G, Low D, Huber T (2013) Origin and differentiation of microglia. Front Cell Neurosci 7:45. [PubMed: 23616747]

Girotti M, Donegan JJ, Morilak DA (2011) Chronic intermittent cold stress sensitizes neuro-immune reactivity in the rat brain. Psychoneuroendocrinology (England) 36:1164–1174.

Gomez Perdiguero E, Klapproth K, Schulz C, Busch K, Azzoni E, Crozet L, Garner H, Trouillet C, de Bruijn MF, Geissmann F, Rodewald HR (2015) Tissue-resident macrophages originate from yolk-sac-derived erythro-myeloid progenitors. Nature 518:547–551 [PubMed: 25470051]

Hashizume H, Horibe T, Ohshima A, Ito T, Yagi H, Takigawa M (2005) Anxiety accelerates T-helper 2-tilted immune responses in patients with atopic dermatitis. Br J Dermatol 152:1161–1164 [PubMed: 15948976]

Heidt T, Sager HB, Courties G, Dutta P, Iwamoto Y, Zaltsman A, von Zur Muhlen C, Bode C, Fricchione GL, Denninger J, Lin CP, Vinegoni C, Libby P, Swirski FK, Weissleder R, Nahrendorf M (2014) Chronic variable stress activates hematopoietic stem cells. Nat Med 20:754–758. [PubMed: 24952646]

Herz J, Filiano AJ, Smith A, Yogev N, Kipnis J (2017) Myeloid Cells in the Central Nervous System. Immunity 46:943–956 [PubMed: 28636961]

Hong M, Zheng J, Ding ZY, Chen JH, Yu L, Niu Y, Hua YQ, Wang LL (2013) Imbalance between Th17 and treg cells may play an important role in the development of chronic unpredictable mild stress-induced depression in mice. Neuroimmunomodulation (Switzerland) 20:39–50.

Hou N, Zhang X, Zhao L, Zhao X, Li Z, Song T, Huang C (2013) A novel chronic stress-induced shift in the Th1 to Th2 response promotes colon cancer growth. Biochem Biophys Res Commun 439:471–476 [PubMed: 24036270]

Hou R, Garner M, Holmes C, Osmond C, Teeling J, Lau L, Baldwin DS (2017) Peripheral inflammatory cytokines and immune balance in Generalised Anxiety Disorder: Case-controlled study. Brain Behav Immun 62:212–218 [PubMed: 28161475]

Hu GZ, Yang SJ, Hu WX, Wen Z, He D, Zeng LF, Xiang Q, Wu XM, Zhou WY, Zhu QX (2016) Effect of cold stress on immunity in rats. Exp Ther Med 11:33–42. [PubMed: 26889214]

Hueston CM, Barnum CJ, Eberle JA, Ferraioli FJ, Buck HM, Deak T (2011) Stress-dependent changes in neuroinflammatory markers observed after common laboratory stressors are not seen following acute social defeat of the Sprague Dawley rat. Physiol Behav 104:187–198 [PubMed: 21406198]

Huse M, Lillemeier BF, Kuhns MS, Chen DS, Davis MM (2006) T cells use two directionally distinct pathways for cytokine secretion. Nat Immunol (United States) 7:247–255.

Inagaki TK, Muscatell KA, Irwin MR, Cole SW, Eisenberger NI (2012) Inflammation selectively enhances amygdala activity to socially threatening images. Neuroimage 59:3222–3226. [PubMed: 22079507]

Kamezaki Y, Katsuura S, Kuwano Y, Tanahashi T, Rokutan K (2012) Circulating cytokine signatures in healthy medical students exposed to academic examination stress. Psychophysiology 49:991–997 [PubMed: 22468981]

Kang HJ, Voleti B, Hajszan T, Rajkowska G, Stockmeier CA, Licznerski P, Lepack A, Majik MS, Jeong LS, Banasr M, Son H, Duman RS (2012) Decreased expression of synapse-related genes and loss of synapses in major depressive disorder. Nat Med (United States) 18:1413–1417.

Karlsson L, Nousiainen N, Scheinin NM, Maksimow M, Salmi M, Lehto SM, Tolvanen M, Lukkarinen H, Karlsson H (2017) Cytokine profile and maternal depression and anxiety symptoms in mid-pregnancy-the FinnBrain Birth Cohort Study. Arch Womens Ment Health 20:39–48 [PubMed: 27699637]

Kaufmann I, Eisner C, Richter P, Huge V, Beyer A, Chouker A, Schelling G, Thiel M (2007) Lymphocyte subsets and the role of TH1/TH2 balance in stressed chronic pain patients. Neuroimmunomodulation 14:272–280. [PubMed: 18239379]

Kettenmann H, Kirchhoff F, Verkhratsky A (2013) Microglia: New roles for the synaptic stripper. Neuron (United States) 77:10–18.

Kiecolt-Glaser JK, Preacher KJ, MacCallum RC, Atkinson C, Malarkey WB, Glaser R (2003) Chronic stress and age-related increases in the pro-inflammatory cytokine IL-6. Proc Natl Acad Sci 100:9090–9095. [PubMed: 12840146]

Kim SJ, Lee H, Lee G, Oh SJ, Shin MK, Shim I, Bae H (2012) CD4+CD25+ regulatory T cell depletion modulates anxiety and depression-like behaviors in mice. PLoS One (United States) 7:e42054.

Kipnis J, Cohen H, Cardon M, Ziv Y, Schwartz M (2004) T cell deficiency leads to cognitive dysfunction: Implications for therapeutic vaccination for schizophrenia and other psychiatric conditions. Proc Natl Acad Sci U S A (United States) 101:8180–8185.

Klapal L, Igelhorst BA, Dietzel-Meyer ID (2016) Changes in neuronal excitability by activated microglia: Differential na(+) current upregulation in pyramid-shaped and bipolar neurons by TNF-alpha and IL-18. Front Neurol (Switzerland) 7:44.

Knapp DJ, Whitman BA, Wills TA, Angel RA, Overstreet DH, Criswell HE, Ming Z, Breese GR (2011) Cytokine involvement in stress may depend on corticotrophin releasing factor to sensitize ethanol withdrawal anxiety. Brain Behav Immun (Netherlands) 25 Suppl 1:S146–54.

Konsman JP, Parnet P, Dantzer R (2002) Cytokine-induced sickness behaviour: Mechanisms and implications. Trends Neurosci 25:154–159. [PubMed: 11852148]

Kraynak TE, Marsland AL, Wager TD, Gianaros PJ (2018) Functional neuroanatomy of peripheral inflammatory physiology: A meta-analysis of human neuroimaging studies. Neurosci Biobehav res 94:76–92

Lapiz-Bluhm MD, Soto-Pina AE, Hensler JG, Morilak DA (2009) Chronic intermittent cold stress and serotonin depletion induce deficits of reversal learning in an attentional set-shifting test in rats. Psychopharmacology (Berl) (Germany) 202:329–341.

Lawson LJ, Perry VH, Dri P, Gordon S (1990) Heterogeneity in the distribution and morphology of microglia in the normal adult mouse brain. Neuroscience 39:151–170. [PubMed: 2089275]

Leitermann RJ, Rostkowski AB, Urban JH (2016) Neuropeptide Y input to the rat basolateral amygdala complex and modulation by conditioned fear. J Comp Neurol 524:2418–2439. [PubMed: 26779765]

Li J, Zhao R, Li X, Sun W, Qu M, Tang Q, Yang X, Zhang S (2016) Shen-qi-jie-yu-fang exerts effects on a rat model of postpartum depression by regulating inflammatory cytokines and CD4(+)CD25(+) regulatory T cells. Neuropsychiatr Dis Treat (New Zealand) 12:883–896.

Liu YY, Zhou XY, Yang LN, Wang HY, Zhang YQ, Pu JC, Liu LX, Gui SW, Zeng L, Chen JJ, Zhou CJ, Xie P (2017) Social defeat stress causes depression-like behavior with metabolite changes in the prefrontal cortex of rats. PLoS One 12:e0176725. [PubMed: 28453574]

Louveau A, Smirnov I, Keyes TJ, Eccles JD, Rouhani SJ, Peske JD, Derecki NC, Castle D, Mandell JW, Lee KS, Harris TH, Kipnis J (2015) Structural and functional features of central nervous system lymphatic vessels. Nature (England) 523:337–341.

Lutgendorf SK, Lamkin DM, DeGeest K, Anderson B, Dao M, McGinn S, Zimmerman B, Maiseri H, Sood AK, Lubaroff DM (2008) Depressed and anxious mood and T-cell cytokine expressing populations in ovarian cancer patients. Brain Behav Immun 22:890–900. [PubMed: 18276105]

Maes M (2011) Depression is an inflammatory disease, but cell-mediated immune activation is the key component of depression. Prog Neuropsychopharmacol Biol Psychiatry (England) 35:664–675.

Maes M, Leonard BE, Myint AM, Kubera M, Verkerk R (2011) The new '5-HT' hypothesis of depression: Cell-mediated immune activation induces indoleamine 2,3-dioxygenase, which leads to lower plasma tryptophan and an increased synthesis of detrimental tryptophan catabolites (TRYCATs), both of which contribute to the onset of depression. Prog Neuropsychopharmacol Biol Psychiatry (England) 35:702–721.

Maes M, Song C, Lin A, De Jongh R, Van Gastel A, Kenis G, Bosmans E, De Meester I, Benoy I, Neels H, Demedts P, Janca A, Scharpé S, Smith RS (1998) The effects of psychological stress on humans: increased production of pro-inflammatory cytokines and a Th1-like response in stress-induced anxiety. Cytokine 10:313–318 [PubMed: 9617578]

Maier SF, Goehler LE, Fleshner M, Watkins LR (1998) The role of the vagus nerve in cytokine-to-brain communication. Ann N Y Acad Sci (United States) 840:289–300.

Marin I, Kipnis J (2013) Learning and memory ... and the immune system. Learn Mem (United States) 20:601–606.

Marsland AL, Walsh C, Lockwood K, John-Henderson NA (2017) The effects of acute psychological stress on circulating and stimulated inflammatory markers: A systematic review and meta-analysis. Brain Behav Immun 64:208–219 [PubMed: 28089638]

McKim DB, Weber MD, Niraula A, Sawicki CM, Liu X, Jarrett BL, Ramirez-Chan K, Wang Y, Roeth RM, Sucaldito AD, Sobol CG, Quan N, Sheridan JF, Godbout JP (2018) Microglial recruitment of IL-1β-producing monocytes to brain endothelium causes stress-induced anxiety. Mol Psychaitry. 23:1421–1431.

Miller AH, Maletic V, Raison CL (2009) Inflammation and its discontents: the role of cytokines in the pathophysiology of major depression. Biol Psychiatry 65:732–741. [PubMed: 19150053]

Miller LG, Galpern WR, Dunlap K, Dinarello CA, Turner TJ (1991) Interleukin-1 augments gamma-aminobutyric acidA receptor function in brain. Mol Pharmacol (United States) 39:105–108.

Miller GE, Chen E, Sze J, Marin T, Arevalo JM, Doll R, Ma R, Cole SW (2008) A functional genomic fingerprint of chronic stress in humans: blunted glucocorticoid and increased NF-kappaB signaling. Biol Psychiatry. 64:266–272 [PubMed: 18440494]

Mormède C, Castanon N, Médina C, Moze E, Lestage J, Neveu PJ, Dantzer R (2002) Chronic mild stress in mice decreases peripheral cytokine and increases central cytokine expression independently of IL-10 regulation of the cytokine network. Neuroimmunomodulation 10:359–366. [PubMed: 12907843]

Morrison H, Young K, Qureshi M, Rowe RK, Lifshitz J (2017) Quantitative microglia analyses reveal diverse morphologic responses in the rat cortex after diffuse brain injury. Sci Rep 7:13211–017–13581–z. [PubMed: 29038483]

Mosmann TR, Sad S (1996) The expanding universe of T-cell subsets: Th1, Th2 and more. Immunol Today 17:138–146. [PubMed: 8820272]

Munshi S, Rosenkranz JA (2018) Effects of Peripheral Immune Challenge on In Vivo Firing of Basolateral Amygdala Neurons in Adult Male Rats. Neuroscience 390:174–186 [PubMed: 30170159]

Nagaraj S, Schrum AG, Cho HI, Celis E, Gabrilovich DI (2010) Mechanism of T cell tolerance induced by myeloid-derived suppressor cells. J Immunol 184:3106–3116 [PubMed: 20142361]

Nakano Y, Nakamura S, Hirata M, Harada K, Ando K, Tabuchi T, Matunaga I, Oda H (1998) Immune function and lifestyle of taxi drivers in Japan. Ind Health 36:32–39. [PubMed: 9473856]

Nakata (2012) Psychosocial job stress and immunity: a systematic review. Methods Mol Biol 934:39–75 [PubMed: 22933140]

National Research Council (2011) Guide for the Care and Use of Laboratory Animals. National Academies Press.

Nelson TE, Olde Engberink A, Hernandez R, Puro A, Huitron-Resendiz S, Hao C, De Graan PN, Gruol DL (2012) Altered synaptic transmission in the hippocampus of transgenic mice with enhanced central nervous systems expression of interleukin-6. Brain Behav Immun (Netherlands) 26:959–971.

Niraula A, Wang Y, Godbout JP, Sheridan JF(2018) Corticosterone production during repeated social defeat causes monocyte mobilization from the bone marrow, glucocorticoid resistance, and neurovascular adhesion molecule expression. J Neurosci 38:2328–2340 [PubMed: 29382712]

Norden DM, Trojanowski PJ, Villanueva E, Navarro E, Godbout JP (2016) Sequential activation of microglia and astrocyte cytokine expression precedes increased iba-1 or GFAP immunoreactivity following systemic immune challenge. Glia (United States) 64:300–316.

Ogoshi F, Yin HZ, Kuppumbatti Y, Song B, Amindari S, Weiss JH (2005) Tumor necrosis-factor-alpha (TNF-alpha) induces rapid insertion of Ca2+-permeable alpha-amino-3-hydroxyl-5-methyl-4-isoxazole-propionate (AMPA)/kainate (ca-A/K) channels in a subset of hippocampal pyramidal neurons. Exp Neurol (United States) 193:384–393.

Ota KT, Liu RJ, Voleti B, Maldonado-Aviles JG, Duric V, Iwata M, Dutheil S, Duman C, Boikess S, Lewis DA, Stockmeier CA, DiLeone RJ, Rex C, Aghajanian GK, Duman RS (2014) REDD1 is essential for stress-induced synaptic loss and depressive behavior. Nat Med (United States) 20:531–535.

Paschall AV, Zhang R, Qi CF, Bardhan K, Peng L, Lu G, Yang J, Merad M, McGaha T, Zhou G, Mellor A, Abrams SI, Morse HC 3rd, Ozato K, Xiong H, Liu K (2015) IFN regulatory factor 8 represses GM-CSF expression in T cells to affect myeloid cell lineage differentiation. J Immunol 194:2369–2379. [PubMed: 25646302]

Passos IC, Vasconcelos-Moreno MP, Costa LG, Kunz M, Brietzke E, Quevedo J, Salum G, Magalhães PV, Kapczinski F, Kauer-Sant'Anna M (2015) Inflammatory markers in post-traumatic stress disorder: a systematic review, meta-analysis, and meta-regression. Lancet Psychiatry 2:1002–1012 [PubMed: 26544749]

Paxinos G, Watson C (1998) The Rat Brain in Stereotaxic Coordinates. Fourth edition. Academic Press, San Diego.

Paxinos G, Watson C (2007) The Rat Brain in Stereotaxic Coordinates. Sixth edition. Academic Press, San Diego.

Plata-Salaman CR, Ffrench-Mullen JM (1992) Interleukin-1 beta depresses calcium currents in CA1 hippocampal neurons at pathophysiological concentrations. Brain Res Bull (United States) 29:221–223.

Powell ND, Sloan EK, Bailey MT, Arevalo JM, Miller GE, Chen E, Kobor MS, Reader BF, Sheridan JF, Cole SW (2013) Social stress up-regulates inflammatory gene expression in the leukocyte transcriptome via beta-adrenergic induction of myelopoiesis. Proc Natl Acad Sci 110:16574–16579. [PubMed: 24062448]

Radjavi A, Smirnov I, Kipnis J (2014) Brain antigen-reactive CD4+ T cells are sufficient to support learning behavior in mice with limited T cell repertoire. Brain Behav Immun (Netherlands) 35:58–63.

Rehm KE, Elci OU, Hahn K, Marshall GD Jr (2013) The impact of self-reported psychological stress levels on changes to peripheral blood immune biomarkers in recreational marathon runners during training and recovery. Neuroimmunomodulation 20:164–176 [PubMed: 23548735]

Renna ME, O'Toole MS, Spaeth PE, Lekander M, Mennin DS (2018) The association between anxiety, traumatic stress, and obsessive-compulsive disorders and chronic inflammation: A systematic review and meta-analysis. Depress Anxiety 35:1081–1094 [PubMed: 30199144]

Rivera C, Li H, Thomas-Crusells J, Lahtinen H, Viitanen T, Nanobashvili A, Kokaia Z, Airaksinen MS, Voipio J, Kaila K, Saarma M (2002) BDNF-induced TrkB activation downregulates the K+-cl– cotransporter KCC2 and impairs neuronal cl– extrusion. J Cell Biol (United States) 159:747–752.

Rosenkranz JA, Venheim ER, Padival M (2010) Chronic stress causes amygdala hyperexcitability in rodents. Biol Psychiatry 67:1128–1136. [PubMed: 20378100]

Rostkowski AB, Teppen TL, Peterson DA, Urban JH (2009) cell-specific expression of Neuropeptide Y Y1 receptor immunoreactivity in the rat basolateral amygdala. J Comp Neurol 16:166–176.

Rygula R, Abumaria N, Domenici E, Hiemke C, Fuchs E (2006) Effects of fluoxetine on behavioral deficits evoked by chronic social stress in rats. Behav Brain Res 174:188–192. [PubMed: 16949682]

Rygula R, Abumaria N, Flugge G, Fuchs E, Ruther E, Havemann-Reinecke U (2005) Anhedonia and motivational deficits in rats: Impact of chronic social stress. Behav Brain Res 162:127–134. [PubMed: 15922073]

Sabharwal L, Kamimura D, Meng J, Bando H, Ogura H, Nakayama C, Jiang JJ, Kumai N, Suzuki H, Atsumi T, Arima Y, Murakami M (2014) The gateway reflex, which is mediated by the inflammation amplifier, directs pathogenic immune cells into the CNS. J Biochem (England) 156:299–304.

Savignac HM, Hyland NP, Dinan TG, Cryan JF (2011). The effects of repeated social interaction stress on behavioural and physiological parameters in a stress-sensitive mouse strain. Behav Brain Res. 216:576–584. [PubMed: 20826188]

Schmitt C, Strazielle N, Ghersi-Egea JF (2012) Brain leukocyte infiltration initiated by peripheral inflammation or experimental autoimmune encephalomyelitis occurs through pathways connected to the CSF-filled compartments of the forebrain and midbrain. J Neuroinflammation (England) 9:187–2094–9–187.

Segerstrom SC, Miller GE (2004) Psychological stress and the human immune system: a meta-analytic study of 30 years of inquiry. Psychol Bull 130: 601–630. [PubMed: 15250815]

Shaashua L, Sominsky L, Levi B, Sorski L, Reznick M, Page GG, Ben-Eliyahu S (2012) In vivo suppression of plasma IL-12 levels by acute and chronic stress paradigms: potential mediating mechanisms and sex differences. Brain Behav Immun 26:996–1005. [PubMed: 22659252]

Shansky RM, Lipps J (2013) Stress-induced cognitive dysfunction: Hormone-neurotransmitter interactions in the prefrontal cortex. Front Hum Neurosci (Switzerland) 7:123.

Shimamiya T, Terada N, Hiejima Y, Wakabayashi S, Kasai H, Mohri M (1985) Effects of 10-day confinement on the immune system and psychological aspects in humans. J Appl Physiol 97:920–924

Slopen N, Loucks EB, Appleton AA, Kawachi I, Kubzansky LD, Non AL, Buka S, Gilman SE (2015) Early origins of inflammation: An examination of prenatal and childhood social adversity in a prospective cohort study. Psychoneuroendocrinology 51:403–413 [PubMed: 25462912]

Stark JL, Avitsur R, Hunzeker J, Padgett DA, Sheridan JF (2002) Interleukin-6 and the development of social disruption-induced glucocorticoid resistance. J Neuroimmunol 124:9–15. [PubMed: 11958817]

Stefanski V, Engler H (1998) Effects of acute and chronic social stress on blood cellular immunity in rats. Physiol Behav 64:733–741 [PubMed: 9817588]

Stefanski V, Knopf G, Schulz S (2001) Long-term colony housing in Long Evans rats: immunological, hormonal, and behavioral consequences. J Neuroimmunol 114:122–130 [PubMed: 11240023]

Stellwagen D, Beattie EC, Seo JY, Malenka RC (2005) Differential regulation of AMPA receptor and GABA receptor trafficking by tumor necrosis factor-alpha. J Neurosci (United States) 25:3219–3228.

Stence N, Waite M, Dailey ME (2001) Dynamics of microglial activation: A confocal time-lapse analysis in hippocampal slices. Glia (United States) 33:256–266.

Stewart AM, Roy S, Wong K, Gaikwad S, Chung KM, Kalueff AV (2015) Cytokine and endocrine parameters in mouse chronic social defeat: implications for translational 'cross-domain' modeling of stress-related brain disorders. Behav Brain Res 276:84–91. [PubMed: 25173699]

Stitt JT(1990) Passage of immunomodulators across the blood-brain barrier. Yale J Biol Med 63: 121 – 131. [PubMed: 2119089]

Strazielle N, Creidy R, Malcus C, Boucraut J, Ghersi-Egea JF (2016) T-lymphocytes traffic into the brain across the blood-CSF barrier: Evidence using a reconstituted choroid plexus epithelium. PLoS One (United States) 11:e0150945.

Stroncek DF, Ren J, Lee DW, Tran M, Frodigh SE, Sabatino M, Khuu H, Merchant MS, Mackall CL (2016) Myeloid cells in peripheral blood mononuclear cell concentrates inhibit the expansion of chimeric antigen receptor T cells. Cytotherapy. 18:893–901. [PubMed: 27210719]

Sugama S, Takenouchi T, Fujita M, Conti B, Hashimoto M (2009) Differential microglial activation between acute stress and lipopolysaccharide treatment. J Neuroimmunol 207:24–31. [PubMed: 19111355]

Tursich M, Neufeld RW, Frewen PA, Harricharan S, Kibler JL, Rhind SG, Lanius RA (2014) Association of trauma exposure with proinflammatory activity: a transdiagnostic meta-analysis. Transl Psychiatry. 4:e413. [PubMed: 25050993]

Tynan RJ, Naicker S, Hinwood M, Nalivaiko E, Buller KM, Pow DV, Day TA, Walker FR (2010) Chronic stress alters the density and morphology of microglia in a subset of stress-responsive brain regions. Brain Behav Immun 24:1058–1068 [PubMed: 20153418]

Urban JH, Leitermann RJ, DeJoseph MR, Somponpun SJ, Wolak ML, Sladek CD (2006) Influence of dehydration on the expression of neuropeptide Y Y1 receptors in hypothalamic magnocellular neurons. Endocrinology 147:4122–4131. [PubMed: 16728491]

Van de Velde LA, Subramanian C, Smith AM, Barron L, Qualls JE, Neale G, Alfonso-Pecchio A, Jackowski S, Rock CO, Wynn TA, Murray PJ (2017) T Cells Encountering Myeloid Cells Programmed for Amino Acid-dependent Immunosuppression Use Rictor/mTORC2 Protein for Proliferative Checkpoint Decisions. J Biol Chem. 292:15–30. [PubMed: 27903651]

van Praag HM (2005) Can stress cause depression? World J Biol Psychiatry 6 Suppl 2:5–22. [PubMed: 16166019]

Vanderschuren LJ, Niesink RJ, Van Ree JM (1997) The neurobiology of social play behavior in rats. Neurosci Biobehav Rev 21: 309–326 [PubMed: 9168267]

Varlinskaya EI, Spear LP (2008) Social interactions in adolescent and adult Sprague-Dawley rats: impact of social deprivation and test context familiarity. Behav Brain Res 188: 398–405 [PubMed: 18242726]

Ver Hoeve ES, Kelly G, Luz S, Ghanshani S, Bhatnagar S (2013) Short-term and long-term effects of repeated social defeat during adolescence or adulthood in female rats. Neuroscience. 249:63–73. [PubMed: 23402852]

Vezzani A, Maroso M, Balosso S, Sanchez MA, Bartfai T (2011) IL-1 receptor/Toll-like receptor signaling in infection, inflammation, stress and neurodegeneration couples hyperexcitability and seizures. Brain Behav Immun (Netherlands) 25:1281–1289.

Vezzani A, Viviani B (2015) Neuromodulatory properties of inflammatory cytokines and their impact on neuronal excitability. Neuropharmacology (England) 96:70–82.

Viviani B, Bartesaghi S, Gardoni F, Vezzani A, Behrens MM, Bartfai T, Binaglia M, Corsini E, Di Luca M, Galli CL, Marinovich M (2003) Interleukin-1beta enhances NMDA receptor-mediated intracellular calcium increase through activation of the src family of kinases. J Neurosci (United States) 23:8692–8700.

Viviani B, Gardoni F, Marinovich M (2007) Cytokines and neuronal ion channels in health and disease. Int Rev Neurobiol (United States) 82:247–263.

Vyas A, Mitra R, Shankaranarayana Rao BS, Chattarji S (2002) Chronic stress induces contrasting patterns of dendritic remodeling in hippocampal and amygdaloid neurons. J Neurosci. 22:6810–6818. [PubMed: 12151561]

Walker FR, Nilsson M, Jones K (2013) Acute and chronic stress-induced disturbances of microglial plasticity, phenotype and function. Curr Drug Targets (United Arab Emirates) 14:1262–1276.

Werneburg S, Feinberg PA, Johnson KM, Schafer DP (2017) A microglia-cytokine axis to modulate synaptic connectivity and function. Curr Opin Neurobiol (England) 47:138–145.

Wohleb ES, Delpech JC (2017) Dynamic cross-talk between microglia and peripheral monocytes underlies stress-induced neuroinflammation and behavioral consequences. Prog Neuropsychopharmacol Biol Psychiatry 79:40–48. [PubMed: 27154755]

Wohleb ES, Fenn AM, Pacenta AM, Powell ND, Sheridan JF, Godbout JP (2012) Peripheral innate immune challenge exaggerated microglia activation, increased the number of inflammatory CNS macrophages, and prolonged social withdrawal in socially defeated mice. Psychoneuroendocrinology 37:1491–1505. [PubMed: 22386198]

Wohleb ES, Franklin T, Iwata M, Duman RS (2016) Integrating neuroimmune systems in the neurobiology of depression. Nat Rev Neurosci (England) 17:497–511.

Wohleb ES, Hanke ML, Corona AW, Powell ND, Stiner LM, Bailey MT, Nelson RJ, Godbout JP, Sheridan JF (2011) β-Adrenergic receptor antagonism prevents anxiety-like behavior and microglial reactivity induced by repeated social defeat. J Neurosci 31:6277–6288. [PubMed: 21525267]

Wohleb ES, McKim DB, Shea DT, Powell ND, Tarr AJ, Sheridan JF, Godbout JP (2014) Re-establishment of anxiety in stress-sensitized mice is caused by monocyte trafficking from the spleen to the brain. Biol Psychiatry. 75:970–981. [PubMed: 24439304]

Wohleb ES, Powell ND, Godbout JP, Sheridan JF (2013) Stress-induced recruitment of bone marrow-derived monocytes to the brain promotes anxiety-like behavior. J Neurosci 33:13820–13833. [PubMed: 23966702]

Wohleb ES, Terwilliger R, Duman CH, Duman RS (2018) Stress-induced neuronal colony stimulating factor 1 provokes microglia-mediated neuronal remodeling and depressive-like behavior. Biol Psychiatry 83:38–49. [PubMed: 28697890]

Woitowich NC, Philibert KD, Leitermann RJ, Wungjiranirun M, Urban JH, Glucksman MJ (2016) EP24.15 as a potential regulator of kisspeptin within the neuroendocrine hypothalamus. Endocrinology 157:820–830. [PubMed: 26653570]

Wu Y, Dissing-Olesen L, MacVicar BA, Stevens B (2015) Microglia: Dynamic mediators of synapse development and plasticity. Trends Immunol (England) 36:605–613.

Yin J-X, Tu J-l, Lin H-j, Shi F-d, Liu R-l, et al. (2010) Centrally administered pertussis toxin inhibits microglia migration to the spinal cord and prevents dissemination of disease in an EAE mouse model. PLoS ONE 5(8): e12400. doi:10.1371/journal.pone.0012400 [PubMed: 20811645]

Yu B, Shinnick-Gallagher P (1994) Interleukin-1 beta inhibits synaptic transmission and induces membrane hyperpolarization in amygdala neurons. J Pharmacol Exp Ther (United States) 271:590–600.

Yuen EY, Wei J, Liu W, Zhong P, Li X, Yan Z (2012) Repeated stress causes cognitive impairment by suppressing glutamate receptor expression and function in prefrontal cortex. Neuron (United States) 73:962–977.

Zhang W, Rosenkranz JA (2012) Repeated restraint stress increases basolateral amygdala neuronal activity in an age-dependent manner. Neuroscience 226: 459–474. [PubMed: 22986163]

HIGHLIGHTS

- Repeated social defeat stress (RSDS) induces anxiety-like behavior

- RSDS increases dual negative but decreases dual positive, CD4+ and regulatory T-cells

- RSDS increases CD4+ and CD8+ T-cells positive for type 2-like profile

- RSDS shifts the balance towards a specific set of T-cells and cytokines

- RSDS activates microglia and increases neuronal firing in the basolateral amygdala
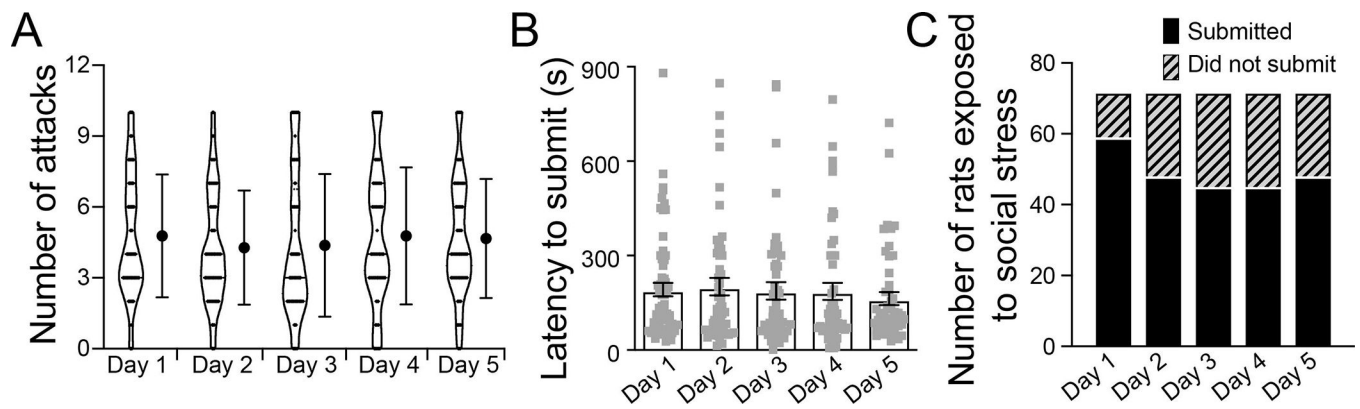
Figure 1: Distribution of rats undergoing social stress across the five days
(A) Number of attacks encountered by the rats undergoing defeat (submission) was similar across all the five days of social stress (Day 1: 4.7 ± 0.3; Day 2: 4.3 ± 0.3; Day 3: 4.4 ± 0.4; Day 4: 4.8 ± 0.3; Day 5: 4.7 ± 0.3; $p = 0.71$, one-way ANOVA). (B) Latency to submit was similar on all the five days (Day 1: 191.9 ± 21.4 s; Day 2: 201.3 ± 27.7 s; Day 3: 188.2 ± 27.8 s; Day 4: 186.2 ± 27.0 s; Day 5: 163.4 ± 20.9 s; $p = 0.874$, one-way ANOVA). (C) Number of rats that did and did not submit to the attacks per day is shown in the bars. Data shown as mean ± S.E.M.

A Open Field Test
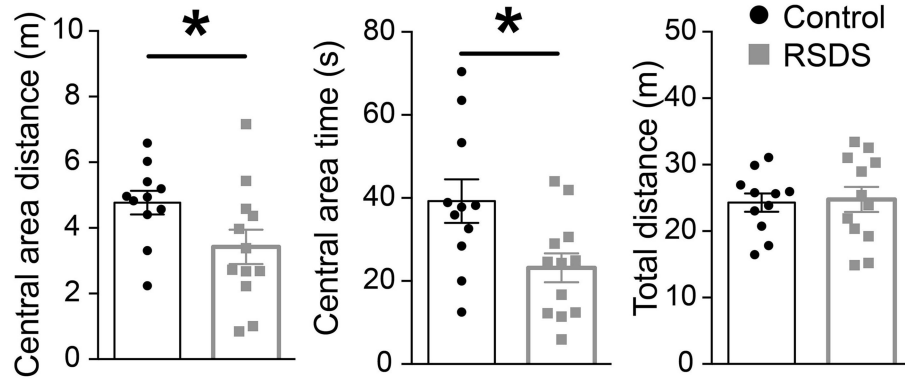
B Social Interaction Test
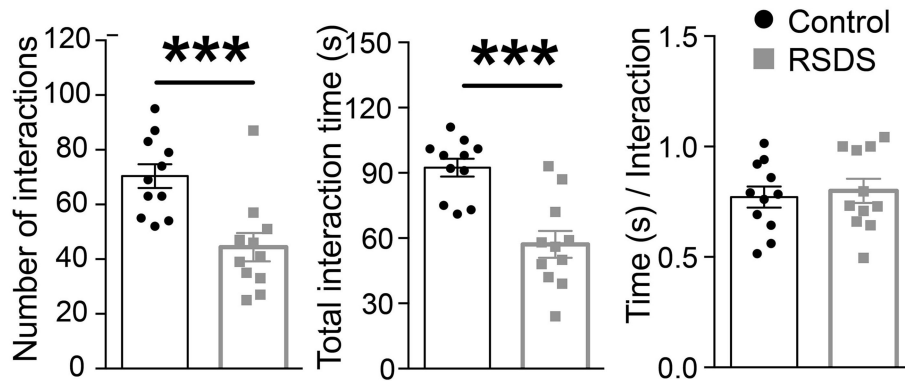
C Elevated Plus Maze Test
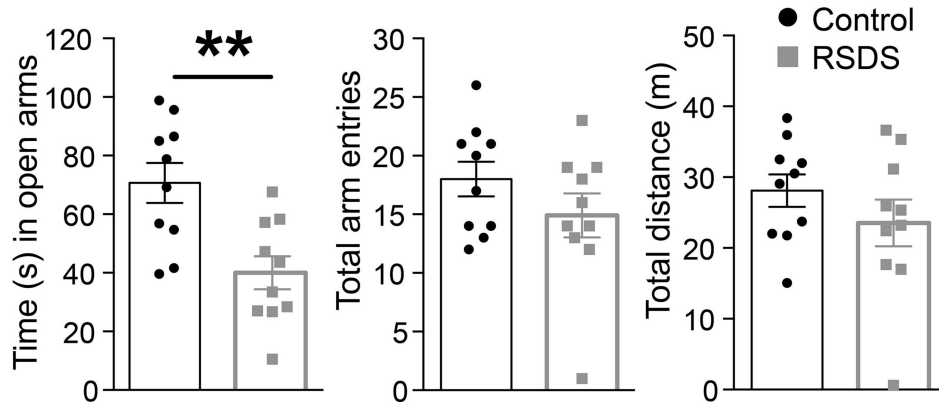
Figure 2: RSDS causes anxiety-like behavior

(A) RSDS decreases central area exploration distance and time without affecting the locomotion (measured by total distance traveled) in OFT. (Left) Central distance: Control: N = 11 rats, 4.76 ± 0.35 m; RSDS: N = 12 rats, 3.42 ± 0.52 m; t = 2.085, df = 21, *p* = 0.04, unpaired *t*-test. (Middle) Central area time: Control: N = 11 rats, 39.23 ± 5.23 s; RSDS: N = 12 rats, 23.16 ± 3.47 s; t = 2.597, df = 21, *p* = 0.01, unpaired *t*-test. (Right) Total distance: Control: N = 11 rats, 24.29 ± 1.37 m; RSDS: N = 12 rats, 24.76 ± 1.89 m; t = 0.198, df = 21, *p* = 0.84, unpaired *t*-test. (B) RSDS decreases number of social interactions. (Left) Number

of social interactions: Control: N = 11 rats, 70.36 ± 4.35; RSDS: N = 11 rats, 44.36 ± 5.19; U = 12.50, p = 0.0008, Mann-Whitney U test. (Middle) Total time of social interactions: Control: N = 11 rats, 92.36 ± 4.10 s; RSDS: N = 11 rats, 57.09 ± 6.17 s; t = 4.756, df = 20, p = 0.0001, unpaired t-test. (Left) Duration of social interactions: Control: N= 11 rats, 0.77 ± 0.04 s; RSDS: N = 11 rats, 0.79 ± 0.05 s; t = 0.387, df = 20, p = 0.70, unpaired t-test. (C) RSDS decreases time spent in open arms of the EPM without affecting locomotion (measured by the total number of arm entries and total distance traveled in EPM). (Left) Time spent in open arms: Control: N = 10 rats, 70.66 ± 6.82 s; RSDS: N = 10 rats, 40.00 ± 5.62 s; t = 3.465, df = 18, p = 0.002, unpaired t-test. (Middle) Total distance traveled: Control: N = 10 rats, 28.09 ± 2.29 m; RSDS: N = 10 rats, 23.53 ± 3.30 m; t = 1.134, df = 18, p = 0.27, unpaired t-test. (Right) Number of arm entries: Control: N = 10 rats, 18.00 ± 1.47; RSDS: N = 10 rats, 14.90 ± 1.87; U = 36, p = 0.30, Mann-Whitney U test. *indicates p < 0.05; **indicates p < 0.01; ***indicates p < 0.001; unpaired t-test (except that for number of interactions, which is by Mann-Whitney U test). Data shown as mean ± S.E.M.
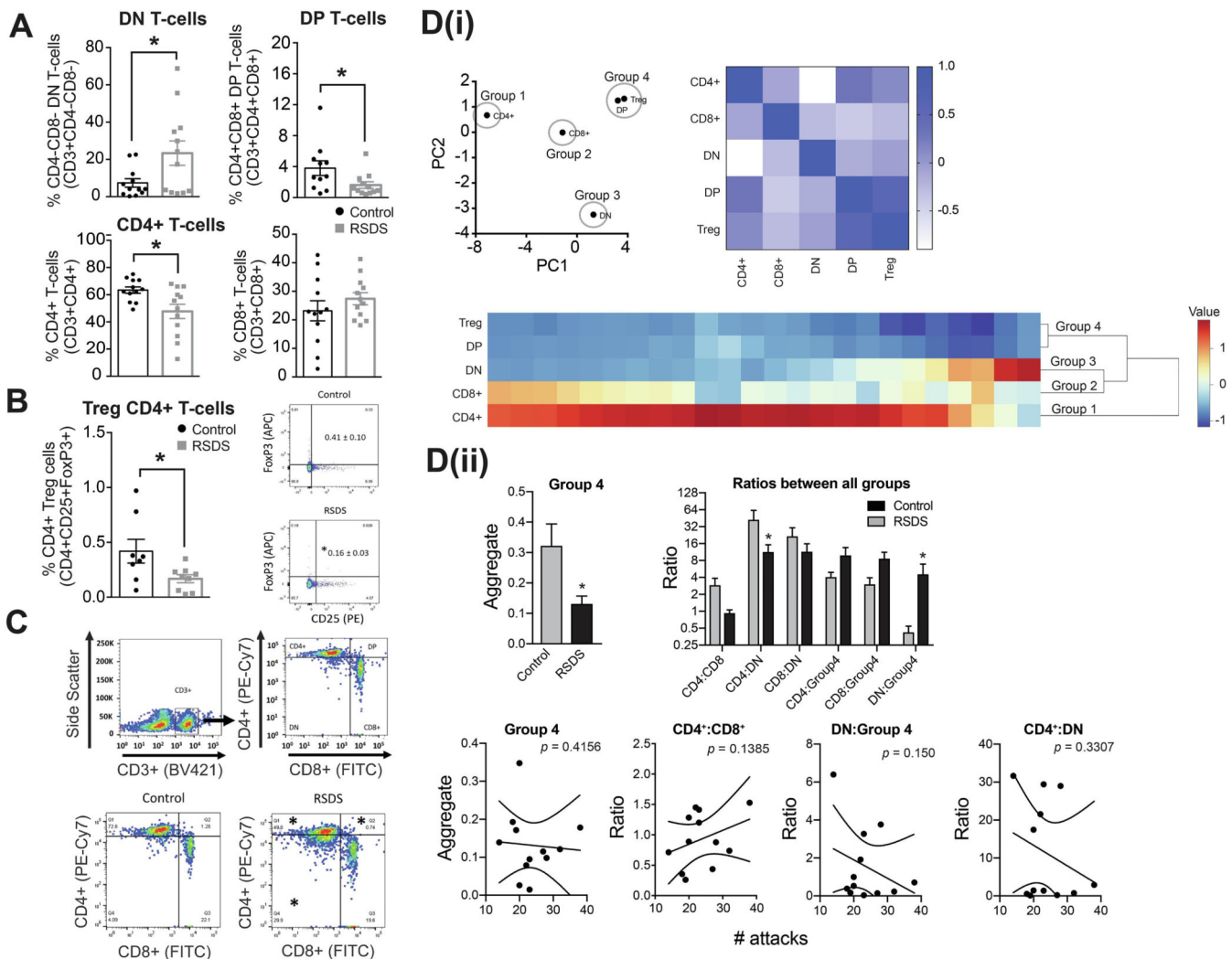
Figure 3: RSDS increases dual-negative (DN) precursor T-cell counts while decreasing dual-positive (DP), mature CD4+ T-cell counts and CD4+ Treg cells

We tested whether RSDS alters the percentage of the T-cell count in peripheral blood (Methods). On the third day after the last session of RSDS or control handling, blood samples were processed with appropriate CD3 (pan T-cell marker), CD4 and CD8 antibodies and analyzed by flow cytometry. Respective isotype controls were run simultaneously to detect any non-specific immunological reactions. (A) Upper left panel: Percentage of DN T-cells are increased by RSDS compared to control. Control: N = 12 rats, 7.36 ± 2.25 %; RSDS: N = 12 rats, 23.35 ± 6.55 %; t = 2.307, df = 22, p = 0.03, unpaired t-test. Upper center-left panel: Percentage of DP T-cells are reduced by RSDS. Control: N = 11 rats, 3.79 ± 0.94; RSDS: N = 12 rats, 1.60 ± 0.42; U = 34, p = 0.04, Mann-Whitney U test. Center-right panel: Percentage of CD4+ T-cells are reduced by RSDS. Control: N = 12 rats, 63.39 ± 2.33 %; RSDS: N = 12 rats, 47.68 ± 5.24 %; t = 2.734, df = 22, p = 0.01, unpaired t-test. Right panel: Percentage of CD8+ T-cells are not altered, but shows a trend towards increase, by RSDS. Control: N = 12 rats, 23.16 ± 3.51 %; RSDS: N = 12 rats, 27.39 ± 2.11 %; t = 1.032, df = 22, p = 0.31, unpaired t-test. * indicates p < 0.05; unpaired t-test. Gating was done for each antibody based on the non-specific binding of the appropriate negative isotype

stained controls. (B) The Treg cells have been defined as CD25+FoxP3+CD4+ T-cells. Left panel: There is a significant decrease of the Treg cells in RSDS group compared to the control (right); Control: N = 8 rats, 0.419 ± 0.108 %; RSDS: N = 9 rats, 0.167 ± 0.036 %; t = 2.316, df = 15, p = 0.03, unpaired t-test. Right panel: CD3+ T-cells have been gated to identify CD25+FoxP3+ cells. Gating was done for each antibody based on the non-specific binding of the appropriate negative isotype stained controls. (C) Upper panel (left and right): Gating strategy used during analysis of single cells by flow cytometry is shown. CD3+ labeled cells were gated as the T-cells, which were further differentiated into dual negative (DN, CD4− CD8−), dual positive (DP, CD4+ CD8+), CD4+ and CD8+ T-cells as shown in the four quadrants. The respective fluorophores used to tag the antibodies have been shown in the parenthesis along the axes. X-axis represents forward scatter while the y-axis indicates side scatter in the plot. Lower panel: Representative scatter plots showing the different population of T-cells after gating from control (left) and RSDS (right) groups. * indicates statistically significant difference ($p < 0.05$; unpaired t-test) from the respective cell population (RSDS vs. control). (Di) PCA analysis was used to group cell types (left). This was followed by correlation matrix to visually confirm that changes in grouped cell types were correlated (right; color bar indicates Pearson r value). The grouping was computationally confirmed with hierarchical clustering analysis (bottom). Based on this analysis, CD4+, CD8+, and dual negative (DN) cells were all independent, and were maintained in separate groups (Groups 1–3). However, dual positive (DP) and Treg cells were highly associated, and were clustered together (Group 4). (Dii) The effect of RSDS on each group was analyzed. Group 1–3 were all comprised of single cell types, so results were the same as (A). RSDS significantly decreased Group 4 (DP and Treg cells; left). The effect of RSDS on the balance between all groups was tested as the ratio between each group pairing. RSDS significantly shifted the balance away from Group 4, and towards DN cells. There was no significant correlation between number of attacks and Groups, nor any of the Ratios, after corrections for multiple comparisons (bottom; correlation examples key measures showns, all $p > 0.05$). Number of attacks indicates the total number of attacks received during the days of defeat. * indicates $p < 0.05$ vs. control. Data shown as mean ± S.E.M.
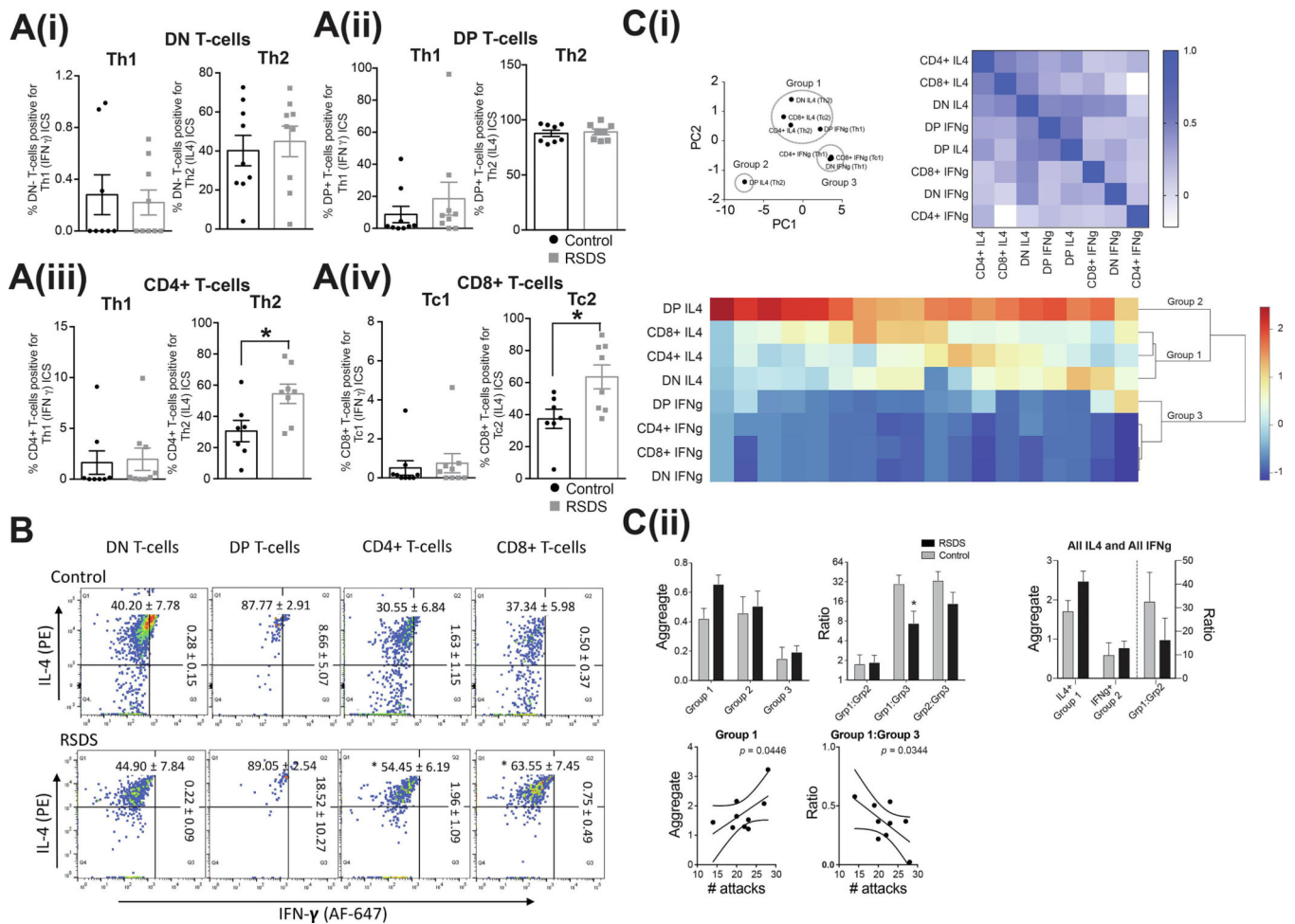
Figure 4: RSDS has no effect on the type 1 (Th1 and Tc1) - positive T-cell counts, but increases type 2 (Th2 and Tc2) - positive mature CD4+ and CD8+ T-cell counts in peripheral blood, in peripheral blood

We tested whether RSDS alters the percentages of Th1 or Tc1 (IFN-γ) positive and Th2 or Tc2 (IL-4) positive T-cell count in peripheral blood. On the third day after the last session of RSDS or control handling, blood samples were processed with appropriate CD3 (pan T-cell marker), CD4, CD8, IFN-γ and IL-4 antibodies, and analyzed by flow cytometry. Respective isotype controls were run simultaneously to detect any non-specific immunological reactions (Methods). (A) Type 1 (Th1/Tc1) or type 2 (Th2/Tc2) intracellular cytokine staining (ICS) profile, measured by IFN-γ or IL-4 staining respectively, of the different T-cell populations, are shown. (Ai) Left shows dual negative Th1 ICS profile: Control: N = 8 rats, 0.280 ± 0.154 %; RSDS: N = 9 rats, 0.220 ± 0.096 %; t = 0.337, df = 15, $p = 0.74$, unpaired t-test. Right shows dual negative: Control: N = 9 rats, 40.20 ± 7.785 %; RSDS: N = 9 rats, 44.90 ± 7.845 %; t = 0.425, df = 16, $p = 0.67$, unpaired t-test. (Aii) Left shows dual positive: Control: N = 9 rats, 8.664 ± 5.071 %; RSDS: N = 9 rats, 18.52 ± 10.27 %; U = 29, $p = 0.33$, Mann-Whitney U test. Right shows dual positive: Control: N = 8 rats, 87.77 ± 2.910 %; RSDS: N = 8 rats, 89.05 ± 2.549 %; U = 29, $p = 0.79$, Mann-Whitney U test. (Aiii) Left shows CD4+ T-cells: Control: N = 8 rats, 1.630 ± 1.158 %; RSDS: N = 9 rats, 1.962 ± 1.098 %; U = 26, $p = 0.34$, Mann-Whitney U test. Right shows

CD4+ T-cells: Control: N = 7 rats, 30.55 ± 6.841 %; RSDS: N = 8 rats, 54.45 ± 6.190 %; t = 2.596, df = 13, p = 0.022, unpaired t-test. (Aiv) Left shows CD8+ T-cells: Control: N = 9 rats, 0.508 ± 0.374 %; RSDS: N = 9 rats, 0.751 ± 0.494 %; U = 35, p = 0.63, Mann-Whitney U test. Right shows CD8+ T-cells: Control: N = 7 rats, 37.34 ± 5.984 %; RSDS: N = 8 rats, 63.55 ± 7.452 %; t = 2.688, df = 13, p = 0.018, unpaired t-test.

Together, the data show that only the CD4+ and CD8+ T-cells positive for Th2 (or Tc2, respectively) cytokines are significantly increased. * indicates $p < 0.05$; unpaired t-test. Gating was done for each antibody based on the non-specific binding of the appropriate negative isotype stained controls. (B) Representative scatter plots from flow cytometric analysis of (A) DN T-cells (B) DP T-cells (C) CD4+ T-cells and (D) CD8+ T-cells are shown. Gating was done for each antibody based on the non-specific binding of the appropriate negative isotype stained controls. (Ci) PCA analysis (left) and correlation matrix (right) support the grouping of T-cells into discrete groups. This was further confirmed with hierarchical clustering analysis, with 3 groups emerging (bottom). (Cii) RSDS had no significant effect on any individual group (left). However, RSDS significantly shifted the balance towards Group 3 (IFNg T-cell), and away from Group 1 (mostly IL4 T-cells; middle). The balance between traditionally defined groups (IL4 or IFNg), with no significant effect of RSDS emerging (right). A significant correlation between number of attacks and Group 1, as well as the balance between Group 1:Group 3, was observed (bottom; p < 0.05 after corrections). Number of attacks indicates the total number of attacks received during the days of defeat. * indicates $p < 0.05$ vs. control. Data shown as mean ± S.E.M.
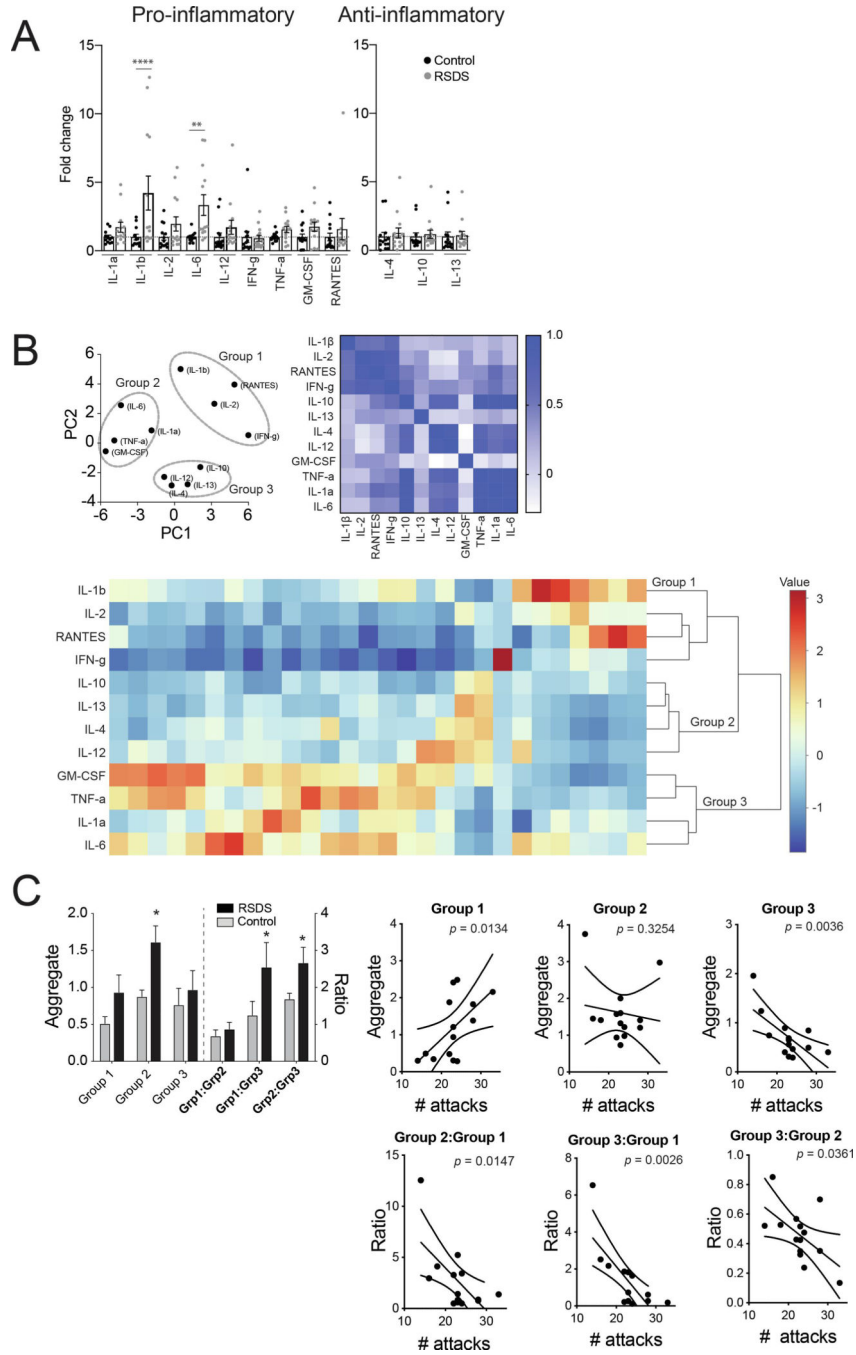
Figure 5: RSDS increases pro-inflammatory, but not anti-inflammatory, cytokine levels in serum
We tested whether RSDS alters serum pro-inflammatory cytokine profiles in peripheral blood. On the third day after the last session of RSDS or control handling, blood samples were collected and processed to obtain serum samples (Methods). (A) Pro-inflammatory cytokine profiles. Fold-changes of different pro-inflammatory cytokines are shown. IL-1β and IL-6 show a significant increase after RSDS compared to control (Bonferroni's multiple comparisons test). **IL-1α** (Control: N = 12 rats, 1.00 ± 0.137; RSDS: N = 13 rats, 1.715 ± 1.317; t = 1.123, $p > 0.05$). **IL-1β** (Control: N = 12 rats, 1.00 ± 0.209; RSDS: N = 13 rats,

4.210 ± 1.242; t = 5.043, ****$p < 0.001$), **IL-2** (Control: N = 14 rats, 1.00 ± 0.222; RSDS: N = 14 rats, 1.953 ± 0.520; t = 1.586, $p > 0.05$). **IL-6** (Control: N = 12 rats, 1.00 ± 0.106; RSDS: N = 13 rats, 3.328 ± 0.758; t = 3.658, **$p < 0.01$), **IL-12** (Control: N = 14 rats, 0.9999 ± 0.293; RSDS: N = 14 rats, 1.710 ± 0.509; t = 1.182, $p > 0.05$), **IFN-γ** (Control: N = 14 rats, 1.000 ± 0.396; RSDS: N = 14 rats, 0.908 ± 0.209; t = 0.1520, $p > 0.05$). **TNF-α** (Control: N = 13 rats, 1.00 ± 0.087; RSDS: N = 14 rats, 1.548 ± 0.224; t = 0.8943, $p > 0.05$). **GM-CSF** (Control: N = 14 rats, 1.00 ± 0.217; RSDS: N = 14 rats, 1.755 ± 0.337; t = 1.257, $p > 0.05$). **RANTES** (Control: N = 14 rats, 1.000 ± 0.277; RSDS: N = 11 rats, 0.802 ± 0.111; t = 0.9181, $p > 0.05$). (B) Anti-inflammatory cytokine profiles. There is no fold-change in the anti-inflammatory cytokine levels after RSDS. **IL-4** (Control: N = 14 rats, 1.000 ± 0.308; RSDS: N = 14 rats, 1.263 ± 0.366; $t = 0.436$, $p > 0.05$, **IL-10** (Control: N = 13 rats, 1.000 ± 0.268; RSDS: N = 14 rats, 1.171 ± 0.293; $t = 0.278$, $p > 0.05$ and **IL-13** (Control: N = 14 rats, 1.000 ± 0.335; RSDS: N = 14 rats, 1.095 ± 0.280; $t = 0.157$, $p > 0.05$.) In this panel, ****indicates $p < 0.0001$, **indicates $p < 0.01$ vs. respective controls; Bonferroni's multiple comparisons test. (B) PCA analysis was used to group cell types (left). This was followed by correlation matrix to visually confirm that changes in grouped cell types were correlated (right; color bar indicates Pearson r value). The grouping was computationally confirmed with hierarchical clustering analysis (bottom). Three groups emerged, Group 1 (IL-1b, IL-2, IFNg, RANTES); Group 2 (IL-1a, IL-6, TNFa, GM-CSF); Group 3 (IL-4, IL-10, IL-12, IL-13).

(C) RSDS significantly increased Group 2 (left), and shifted the balance away from Group 3, towards Group 1 and Group 2. The correlations between the number of attacks and key measures is shown here (right), with significant correlations between attacks and Group 1, and Group 3 ($p < 0.05$ after correlations), and between attacks and the balances between all groups ($p < 0.05$ after correlations). Number of attacks indicates the total number of attacks received during the days of defeat. * indicates $p < 0.05$ vs. control. Data shown as mean ± S.E.M.
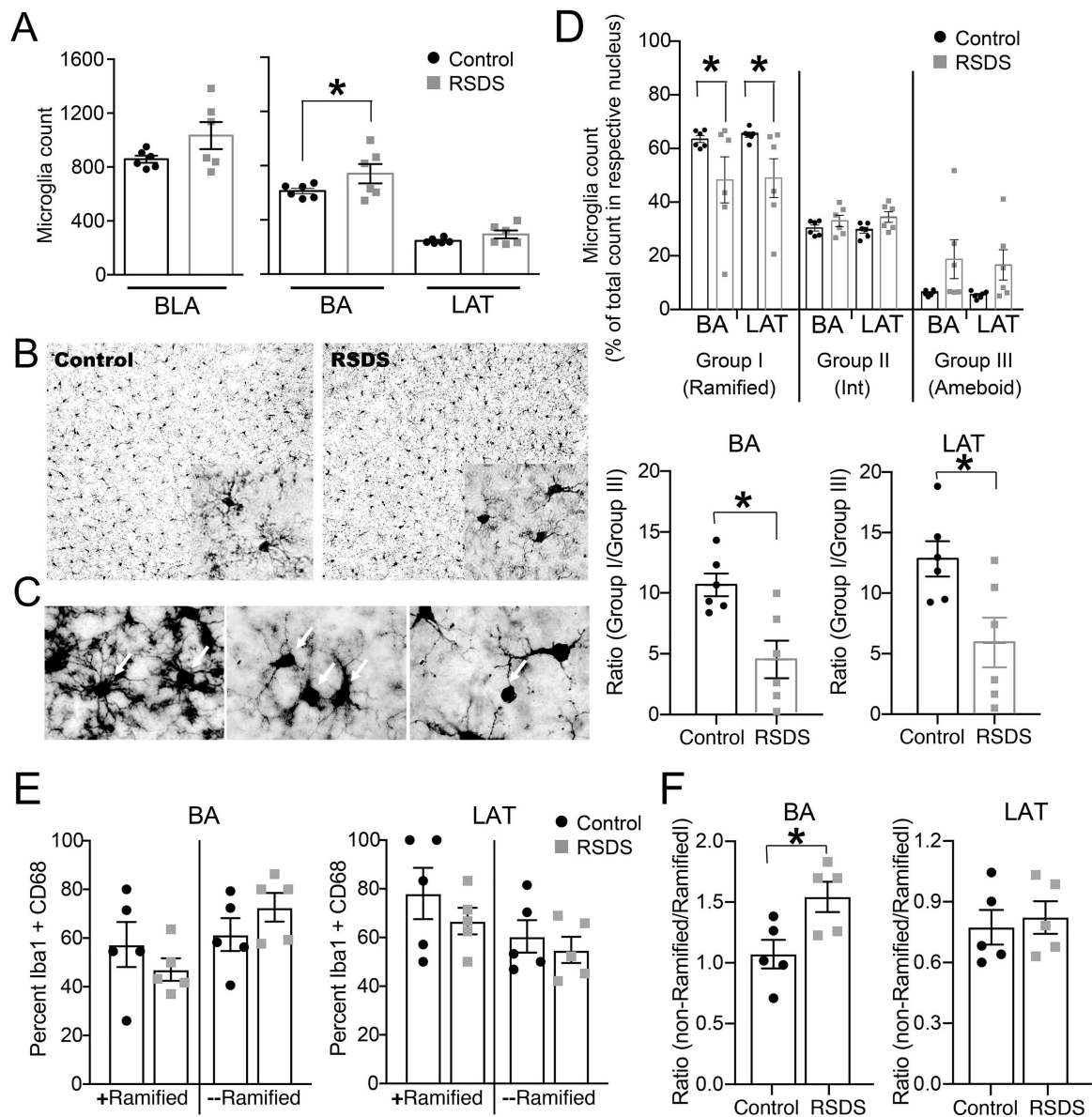
Figure 6: RSDS increases microglia count in the BA nuclei of BLA and causes microglial activation in BLA

Rats were exposed to RSDS or control handling. Microglia were identified by staining with Iba-1 antibody by immunohistochemistry of rat brain sections containing BLA (Methods). (A) Left panel: Microglia count shows a trend towards increase in the BLA (Control: 857.8 ± 26.28 / 6 rats, RSDS: 1033 ± 100.4 / 6 rats; $t = 1.689$, df = 10, $p = 0.122$, unpaired t-test). Right panel: Microglia count is increased in the BA nucleus ($p = 0.035$; Control: 612.8 ± 19.90 / 6 rats, RSDS: 740.4 ± 71.08 / 6 rats) but is unchanged in the LAT nuclei ($p = 0.408$; Control: 245.0 ± 7.823 / 6 rats, RSDS: 292.6 ± 29.37 / 6 rats). (B) Representative images from control and RSDS groups showing the microglia under 20X magnification. Inset shows image in 100X objective lens magnification. (C) Different morphologies of microglia are shown by respective white arrows. Left: Group I (ramified) microglia. Middle: Group II (intermediate) microglia. Right: Group III (ameboid) microglia. (D) Upper panel:

Stress shifted the proportion of microglia types (stress × microglia group interaction, p = 0.042, F(6,40) = 2.433, two-way RM-ANOVA), with a decrease in Group I microglia in the BA and in the LAT (p<0.05, post hoc Bonferroni multiple comparisons test). Lower panel: The ratio of Group I/Group III microglia was shifted after stress compared to controls for both BA (t = 3.39, DF = 10, p = 0.007) and LAT (t = 2.741, DF = 10, p = 0.021). (E) Stress did not consistently impact the percent of cells double-labeled for Iba-1 and CD68 in the BA (left; stress × microglia interaction, p = 0.67, F(1,8) = 0.197; main effect of stress, p = 0.33, F(1,8) = 1.10, two-way ANOVA, n = 5 rats/group), or LAT (right; stress × microglia interaction, p = 0.28, F(1,8) = 1.33; main effect of stress, p = 0.84, F(1,8) = 0.04, two-way ANOVA, n = 5 rats/group). (F) Stress shifted the percent of cells that were double-labeled and minimally ramified relative to double-labeled ramified cells in the BA (p = 0.025, t = 2.744, df = 8, two-tailed unpaired t-test), with no consistent effect in the LAT (p = 0.69, t = 0.41, df = 8, two-tailed unpaired t-test). Values indicate mean ± S.E.M. * indicates $p < 0.05$.
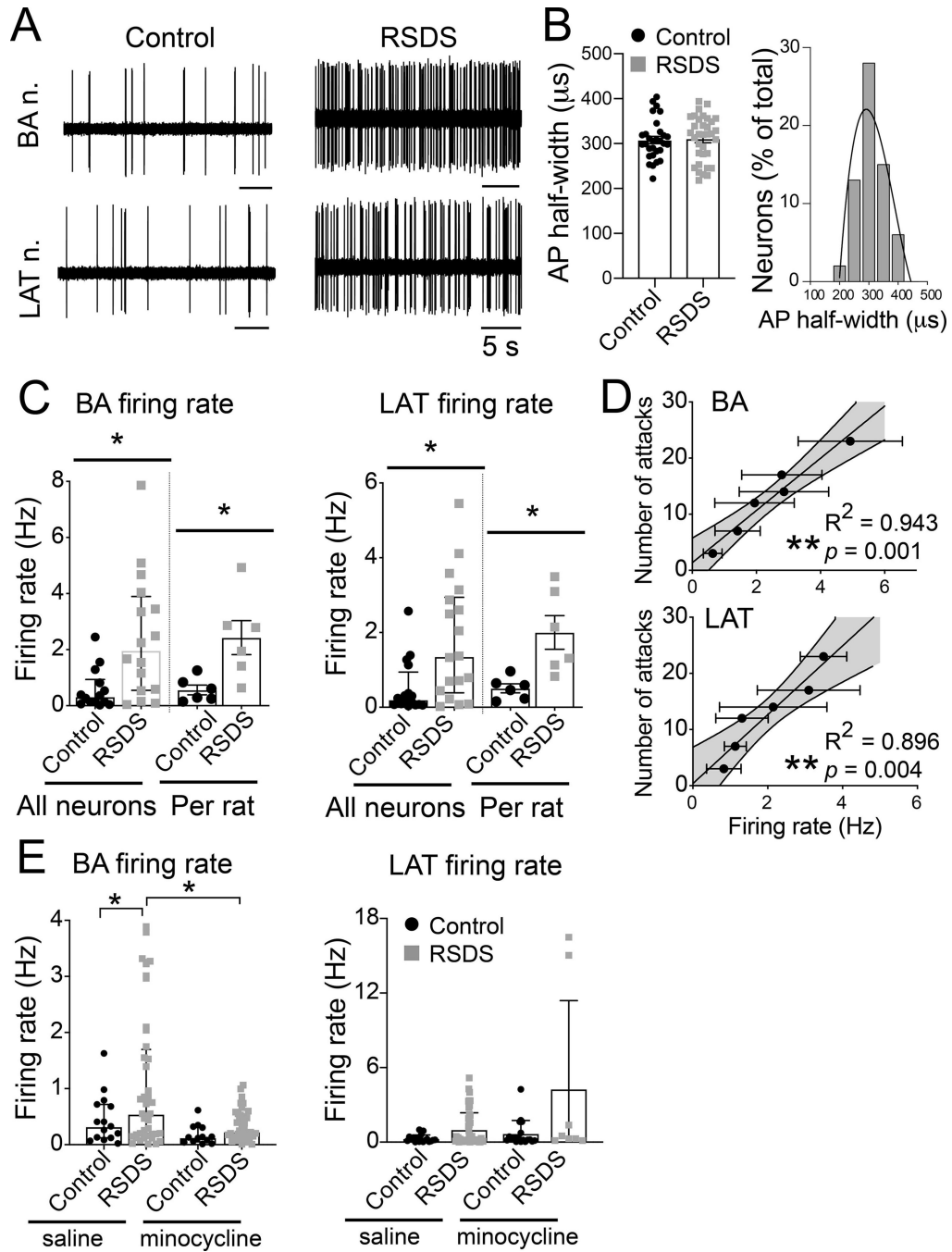
Figure 7: RSDS increases neuronal firing in BA and LAT nuclei of BLA similarly

Rats were exposed to RSDS or control handling, and the neuronal firing was recorded using *in vivo* single-unit extracellular electrophysiology (Methods). (A) Representative traces of electrophysiological recordings from BA (upper panel) and LAT (lower panel) nuclei. (B) AP half-width was similar in the control and RSDS groups. Right: Frequency distribution of the AP half-width from all the recorded BLA neurons show a single population, likely pyramidal neurons. N = 6 rats / group; likely projection neurons, based on action potential half-width; Control 307.8 ± 8.0 μs, n = 30 neurons, RSDS 310.6 ± 8.5 μs, n = 34 neurons; *p*

(RSDS vs. Control) = 0.813; unpaired *t*-test; BA 320.4 ± 8.0 μs, n = 30 neurons; LAT 299.6 ± 8.2 μs, n = 34 neurons. BA: Control 0.59 ± 0.19 Hz, n = 14 neurons; RSDS 2.44 ± 0.55 Hz, n = 16 neurons; U = 46.50, *p* = 0.0054, Mann-Whitney *U* test. LAT: Control 0.52 ± 0.18 Hz, n = 16 neurons; RSDS 1.78 ± 0.38 Hz, n = 18 neurons; U = 69.50, *p* = 0.0090, Mann-Whitney *U* test. (C) Firing rate was significantly increased after RSDS in BA (left) and LAT (right). Data of individual firing rate from all neurons (median ± interquartile range) and those averaged per rat is shown. (D) Significant correlation between the number of attacks and firing rate was seen in both the BA (top) and LAT (bottom) nuclei of RSDS rats. Number of attacks indicates the total number of attacks received during all 5 days of defeat. (E) Blockade of microglia activation by minocycline diminished the firing rate of neurons in the repeated stress condition for BA (left) but not LAT (right). Control-saline N = 7 rats; control-minocycline N = 5 rats; stress-saline N = 11 rats; stress-minocycline N = 7 rats. Minocycline reduced the effects of repeated stress on BA neuron firing (main effect *p* = 0.039, F(1,127) = 4.35, two-way ANOVA; control-saline n = 15 neurons, control-minocycline n = 16 neurons, stress-saline n = 49 neurons, stress-minocycline n = 51 neurons), but did not exert consistent effects on LAT neuron firing (main effect *p* = 0.162, F(1,81) = 1.99; control-stress n = 14 neurons, control-minocycline n = 18 neurons, stress-saline n = 48 neurons, stress-minocycline n = 8 neurons). Values plotted are mean ± SEM unless otherwise noted above. Shaded area indicates 95% confidence intervals. * indicates *p* < 0.05; ** indicates *p* < 0.01.